

BOLT-GAN: Bayes-Optimal Loss for Stable GAN Training

Mohammadreza Tavasoli Naeini
University of Toronto

mohammadreza.tavasolinaeini@mail.utoronto.ca

Ali Bereyhi
University of Toronto

ali.bereyhi@utoronto.ca

Morteza Noshad
Stanford University

noshad@stanford.edu

Ben Liang
University of Toronto

liang@ece.utoronto.ca

Alfred O. Hero III
University of Michigan

hero@eecs.umich.edu

Abstract

We introduce BOLT-GAN, a simple yet effective modification of the WGAN framework inspired by the Bayes optimal learning threshold (BOLT). We show that with a Lipschitz continuous discriminator, BOLT-GAN implicitly minimizes a different metric distance than the Earth-Mover (Wasserstein) distance, and also has better training stability. Empirical evaluations on four standard image-generation benchmarks, (CIFAR-10, CelebA-64, LSUN Bedroom-64, and LSUN Church-64) show that BOLT-GAN consistently outperforms WGAN, achieving 10-60% lower Fréchet Inception Distance (FID). Our results suggest that BOLT is a broadly applicable principle for enhancing GAN training. The software is available in our anonymous repository.

1 Introduction

The Bayes optimal learning threshold (BOLT) (Naeini et al., 2025) is a recently proposed framework for discriminative learning. In its basic form, BOLT develops a computational approach to estimate the Bayes error rate, i.e., the lowest classification error achievable by a representation, by sampling an arbitrary learning model. This introduces the *BOLT loss*, whose minimization drives the model toward the Bayes optimal classifier.

This work adapts the BOLT framework to generative modeling by training the discriminator of a generative adversarial network (GAN) via the BOLT loss. We treat the GAN discriminator as a binary classifier and train it using the BOLT framework. Under this framework, the BOLT objective recovers the well-known Wasserstein GAN (WGAN) (Arjovsky et al., 2017) formulation, up to a minor adjustment: the discriminator outputs are constrained to a bounded range. This perspective provides both a Bayesian interpretation of adversarial learning and a pathway to improve training stability. Building on this foundation, we propose the *BOLT-GAN*, which inherits WGAN-style convergence guarantees while driving discriminator performance toward Bayes optimality.

1.1 Background and Related Work

Bayes Error Estimation The Bayes error rate is a central concept in statistical learning, characterizing the minimum error of a classification task (Bishop, 2006). Classical approaches estimate this error rate via distance-based measures such as Bhattacharyya or Mahalanobis distances (Bhattacharyya, 1943; Mahalanobis, 1936). These methods often fail in high dimensions (Devroye et al., 1996). More recent methods

employ nonparametric or model-based estimators, such as k -nearest neighbors (Moon et al., 2017) or ϵ -ball techniques (Noshad et al., 2019). The BOLT framework (Naeini et al., 2025) provides a unifying alternative, deriving a bound on Bayes error from classifier outputs and introducing a loss that aligns learning with approximation of the Bayes optimal classifier.

GAN GAN (Goodfellow et al., 2014) consists of a generator, which synthesizes data samples from a latent variable, and a discriminator, which distinguishes between real and generated samples. It is trained via a min-max game between the generator and discriminator. While powerful, the original formulation based on Jensen–Shannon divergence is unstable (Goodfellow et al., 2014; Arjovsky et al., 2017). Numerous alternatives have been proposed: Wasserstein GAN (WGAN) (Arjovsky et al., 2017) leverages the Lipschitz continuity of the discriminator to improve gradient backpropagation. This is implemented by approaches such as WGAN-GP (Gulrajani et al., 2017) which enforce the Lipschitz constraint via gradient penalty. Other variants include f -GAN (Nowozin et al., 2016), which generalizes the objective to any f -divergence, LS-GAN (Mao et al., 2017), BEGAN (Berthelot et al., 2017), and techniques such as spectral normalization (Miyato et al., 2018) or progressive growing (Karras et al., 2018). These lines of work aim to stabilize training, but do not try to achieve statistical optimality.

Statistical and Bayesian Perspectives The GAN has been studied from many statistical or Bayesian viewpoints. Bayesian GANs (Saatchi and Wilson, 2017; Ye and Zhu, 2018) introduce uncertainty quantification by estimating posterior distribution. Others, such as (Zhang et al., 2021; Arora et al., 2017), analyze GAN training through the lens of generalization and statistical distances. Our paper adds to this line of study by describing the GAN discriminator explicitly as a model-free Bayes-aligned classifier. In doing so, we provide a Bayesian perspective for adversarial learning and introduce a learning objective function, the bolt loss, for learning a representation that minimize the classification error.

1.2 Main Contributions

The key contributions of this work are as follows: *(i)* We introduce *BOLT-GAN*, an adversarial framework in which the discriminator is trained with the BOLT loss. The generator is implicitly trained to maximize the Bayes error of discrimination task. The inner maximization identifies the Bayes-aligned discriminator with the largest real-fake gap, and the outer minimization drives the generator to reduce this gap, effectively pushing the Bayes error toward random guessing. *(ii)* We characterize convergence of the BOLT-GAN. We show that, under balanced class priors, the BOLT objective is directly linked to total variation (TV) between the data and generator distributions. This finding shed lights on the numerical instability of the plain BOLT-GAN training algorithm. *(iii)* To address this instability issue, we propose Lipschitz BOLT-GAN, which enforces a 1-Lipschitz constraint on the discriminator. We show that under this constraint, the learning objective is bounded above Wasserstein distance. This indicates that this framework guides the generator toward the data distribution using a weaker notion of distance. This leads to stabilization of the gradient backpropagation. *(iv)* We validate our results empirically. On CIFAR-10, CelebA-64, and LSUN, Lipschitz BOLT-GAN showing significant improvements.

Notation Throughout the paper, we adapt the following notation: expectations of of a random variable X with respect to a distribution P is denoted by $\mathbb{E}_{X \sim P}[\cdot]$. The distribution $P = P_C$ is defined as the conditional data distribution given the class C. The set $\{1, \dots, n\}$ is abbreviated as $[n]$.

2 Background and Preliminaries

We restrict our analysis to a binary classification task with classes C_1 and C_2 , although extensions to multi-class problems are possible. Consider a binary classification task with classes C_1 and C_2 occurring with prior probabilities q_1 and $q_2 = 1 - q_1$, respectively. The data samples are drawn from the space $\mathcal{X} \subseteq \mathbb{R}^d$, for some integer d , with class-conditional distributions P_1 and P_2 for the classes C_1 and C_2 , respectively. For this setting, the *Bayes error rate (BER)*, denoted by $\varepsilon_{\text{Bayes}}$, is defined as the minimum error probability achievable by a measurable classifier $f : \mathcal{X} \mapsto \{C_1, C_2\}$. The BER is determined from the data distribution

as (Bishop, 2006)

$$\varepsilon_{\text{Bayes}} = 1 - \int_{\mathcal{X}} \max_{\lambda} [q_{\lambda} P_{\lambda}(x)] \, dx. \quad (1)$$

and is achieved by the maximum a posteriori (MAP) classifier, which assigns a sample x to the class $\lambda \in \{1, 2\}$ that maximizes the joint distribution $q_{\lambda} P_{\lambda}(x)$.

2.1 BOLT Loss for Classification

An explicit computation of the BER(1) requires full knowledge of the data distribution, i.e., both the class prior q_{λ} and the class conditional feature distribution P_{λ} . As these are unavailable, the BER must be bounded and/or estimated ; see (Devroye et al., 1996; Fukunaga, 2013; Noshad et al., 2019) for some sample studies. The recent study by Naeini et al. (2025) develops a new framework to estimate an *upper bound* on the Bayes error. The bound is *universal* in the sense that it can be computed by sampling from an arbitrary measurable and bounded function, e.g., a neural network. It is further *tight*, as it can achieve the Bayes error when optimized over a set of measurable functions. Motivated by these observations, Naeini et al. (2025) introduces the BOLT loss, which utilizes the proposed bound to approximate the optimal Bayes classifier via a parameterized learning model.

Theorem 1 (Binary Bayes error (Naeini et al., 2025)). *Let $h : \mathcal{X} \rightarrow [-1, 0]$ be a measurable function. Then, the Bayes error of the binary classification satisfies*

$$\varepsilon_{\text{Bayes}} \leq q_2 + q_2 \mathbb{E}_{X \sim P_2} [h(X)] - q_1 \mathbb{E}_{X \sim P_1} [h(X)]. \quad (2)$$

Naeini et al. (2025) show that the bound (2) is tight when optimized over h . This enables a computational means to estimate $\varepsilon_{\text{Bayes}}$ by sampling from output of classifier. In particular if h is a parameterized predictor model $h_{\theta}(\cdot)$, e.g., a neural network with weights θ , the bound can be estimated and minimized. This transforms the upper bound in Theorem 1 into a training objective referred to as the Bayes optimal learning threshold (BOLT). While Naeini et al. (2025) establish the BOLT loss for a general multi-class problem, in this work we focus on the binary case, relevant to the discrimination component of the GANs.

Training via BOLT Consider a training dataset $\mathcal{D} = \{(x_i, \lambda_i) : i \in [n]\}$, where $\lambda_i \in \{1, 2\}$ denotes the class index from which x_i is drawn. Assume that the samples in \mathcal{D} are drawn i.i.d. from the data distribution. BOLT trains a parameterized model $h_{\theta} : \mathcal{X} \rightarrow [-1, 0]$ on the dataset \mathcal{D} to estimate the Bayes error rate by optimizing BER empirical loss over θ .

Remark 1. *Note that the output of the model h_{θ} is restricted to be within the interval $[-1, 0]$. This is not a significant restriction, as it corresponds to a simple negation of the softmax output of the classifier.*

For a given sample $(x, \lambda) \in \mathcal{D}$, the BOLT loss is defined as

$$\ell_{\text{BOLT}}(h_{\theta}(x), \lambda) = (-1)^{\lambda} h_{\theta}(x). \quad (3)$$

To train the model h_{θ} on \mathcal{D} , where the empirical risk

$$\hat{R}(\theta) = \frac{1}{n} \sum_{i \in [n]} \ell_{\text{BOLT}}(h_{\theta}(x_i), \lambda_i), \quad (4)$$

This minimization can be done by mini-batch stochastic gradient descent or other standard training method.

The connection, between the BOLT-trained model and the Bayes error rate, can be understood using the results of Naeini et al. (2025): from Theorem 1, we can write

$$\varepsilon_{\text{Bayes}} \leq q_2 + \mathbb{E} [\ell_{\text{BOLT}}(h_{\theta}(X), \lambda)], \quad (5)$$

where the expectation is taken with respect to the data distribution. Note that the prior q_2 is efficiently estimated from the data. By universal approximation (Cybenko, 1989) and the tightness result of Naeini et al. (2025), one can conclude that the trained model in this case efficiently estimates the Bayes error.

2.2 Generative Adversarial Networks

A GAN consists of two learning models: a generator g_ϕ that generates data samples from the latent variable¹ $Z \sim P_Z$ to generate samples of an estimator of \mathcal{X} , and a discriminator h_θ that distinguishes the generated sample $g_\phi(Z)$ from the true data sample $X \sim P_{\text{data}}$. To keep the notation tractable, we denote the induced distribution, i.e., distribution of $g_\phi(Z)$, by P_g , which is determined by P_Z and the generator model g_ϕ .

From a learning perspective, the discriminator solves a binary classification problem: it classifies the input as $C = \text{real}$ or $C = \text{fake}$, corresponding to $\lambda = 1$ or $\lambda = 2$. The conventional approach is to train h_θ such that it estimates the posterior class probability. This leads to the *vanilla GAN* design proposed by Goodfellow et al. (2014). An alternative approach is to use the Kantorovich-Rubinstein duality (Villani et al., 2009) to implicitly minimize the Wasserstein distance between the data and induced distributions. This approach leads to the *Wasserstein GAN* design (Arjovsky et al., 2017). We briefly explain these two approaches in the sequel.

Vanilla GAN The vanilla training approach, proposed in the initial study by Goodfellow et al. (2014), treats the discrimination as a classic binary classification problem. In this sense, it sets $h_\theta(x) = P(C = \text{real}|x)$ and uses the cross-entropy loss to train it.² This approach implicitly implements the maximum likelihood training of the generator (Arjovsky et al., 2017). The risk function, i.e., the expected loss used for training, in this case is given by

$$R_{\text{ML}}(\phi, \theta) = \mathbb{E} [\text{CE}(Y, \lambda)], \quad (6)$$

where CE denotes the cross-entropy loss function, Y is the output of the discriminator, i.e., $Y = h_\theta(X)$, for an input $X \in \mathcal{X}$ to the discriminator, and $\lambda \in \{1, 2\}$ is the label of X with $\lambda = 1$ and $\lambda = 2$ denoting **real** and **fake** inputs respectively. Where λ is sampled from a prior $\pi = \Pr \{\lambda = 1\}$ for some $\pi \in (0, 1)$,³ and X is sampled conditionally from $P_1 = P_{\text{data}}$ when $\lambda = 1$ and $P_2 = P_g$ when $\lambda = 2$.

Noting that $P_2 = P_g$ is the distribution of $g_\phi(Z)$ computed from the latent sample $Z \sim P_Z$, we can use the definition of cross-entropy to expand the risk (6) as

$$\begin{aligned} R_{\text{ML}}(\phi, \theta) = & -\pi \mathbb{E}_{X \sim P_{\text{data}}} [\log h_\theta(X)] \\ & - (1 - \pi) \mathbb{E}_{Z \sim P_Z} [\log(1 - h_\theta(g_\phi(Z)))] . \end{aligned} \quad (7)$$

Defining $\mathcal{L}_{\text{ML}}(\phi, \theta) = -R_{\text{ML}}(\phi, \theta)$, the generator and discriminator are jointly trained by the following min-max game

$$\min_{\phi} \max_{\theta} \mathcal{L}_{\text{ML}}(\phi, \theta), \quad (8)$$

which is equivalent to the *worst-case risk* minimization, i.e., fooling the best discriminator. It is shown that the solution to this min-max game, when solved for any measurable generator g and discriminator h , guarantees the convergence of P_g to P_{data} as measured by the convergence of the Jensen–Shannon (JS) divergence to zero (Goodfellow et al., 2014, Theorem 1).

Wasserstein GAN Arjovsky et al. (2017) propose to train the generator-discriminator pair by minimizing the Wasserstein-1 distance, also known as Earth Mover (EM) distance, between P_{data} and P_g . Using the Kantorovich-Rubinstein duality, it is shown that the EM distance minimization is equivalent to solving a min-max problem with the following objective (Arjovsky et al., 2017, Theorem 3)

$$\begin{aligned} \mathcal{L}_{\text{EM}}(\phi, \theta) = & \mathbb{E}_{X \sim P_{\text{data}}} [h_\theta(X)] \\ & - \mathbb{E}_{Z \sim P_Z} [h_\theta(g_\phi(Z))] . \end{aligned} \quad (9)$$

The training is carried out by solving the same min-max game as in (8) with $\mathcal{L}_{\text{EM}}(\phi, \theta)$ as the objective. While the WGAN still guarantees the convergence of P_g to P_{data} , the notion of convergence is *weaker* than

¹Typically, Z is drawn from a multivariate Gaussian distribution.

²In practice, h_θ is a network with sigmoid-activated output.

³Typically, $\pi = 0.5$ is considered.

vanilla GAN, in the sense that it only minimizes the EM distance between the two distributions instead of an information divergence. Arjovsky et al. (2017) show that the WGAN has better training stability, as compared with the vanilla GAN approach.

Remark 2. Note that in the WGAN, the discriminator model h_θ is not restricted to compute probabilities. Intuitively, The discriminator in this case is a real-valued critic rather than a probabilistic classifier. The model h_θ is however constrained to be 1-Lipschitz. In practice, this constraint can be enforced by approaches such as weight clipping, gradient penalty, or spectral normalization. See the supplementary file for additional discussion.

3 BOLT-GAN Framework

Here we develop the proposed BOLT-GAN framework for training a GAN model. This scheme invokes the BOLT loss to train the generator to fool the Bayes optimal discriminator. The convergence in BOLT-GAN is in the sense of convergence in total variation, i.e., stronger than vanilla GAN, for a Lipschitz discriminator it converges in a weaker sense than WGAN. This implies a trade-off between the strength of convergence and stability.

3.1 MAP Estimator via BOLT

To understand the BOLT-GAN framework, we first present a result which relates a BOLT-trained model to the Bayesian optimal classifier: consider $h_\theta : \mathcal{X} \rightarrow [-1, 0]$ that is trained for a binary classification task using the BOLT loss. Theorem 2 shows how an estimator of the Bayesian optimal classifier, i.e., the MAP estimator, is computed from h_θ .

Theorem 2 (BOLT Estimator of MAP Classifier). *Let h^* be the minimizer of the upper bound in Theorem 1. Assume that the model h_θ approximates h^* in the sense that $\|h^*(x) - h_\theta(x)\|_\infty \leq \epsilon$. Then, the plug-in classifier*

$$\hat{C}_\theta(x) = \begin{cases} C_1 & h_\theta(x) \geq -0.5, \\ C_2 & h_\theta(x) < -0.5. \end{cases} \quad (10)$$

is a plug-in estimator of the MAP classifier, i.e.

$$\hat{C}(x) = \arg \max_{\lambda \in \{1, 2\}} q_\lambda P_\lambda(x) \quad (11)$$

Proof. The proof is given in the supplementary file. □

Remark 3 (BOLT Bias and Variance). *Let $U(x)$ denote the likelihood ratio $U(x) = P_1(x)/P_2(x)$ and let \hat{U} be its plug-in estimator (see the supplementary file for construction details). Assume $\mathbb{E}[|\hat{U}(X) - U(X)|] \leq \varepsilon_0$. Then the BOLT plug-in Bayes-error estimator satisfies*

$$|\mathbb{E}[\hat{\varepsilon}_{\text{BOLT}}] - \varepsilon_{\text{Bayes}}| \leq q_1 \varepsilon_0 + \mathcal{O}(M^{-1/2}), \quad (12)$$

$$\text{Var}(\hat{\varepsilon}_{\text{BOLT}}) = \mathcal{O}(M^{-1}), \quad (13)$$

where M is the number of samples used in the plug-in estimator. Additional details are given in the supplementary file.

Theorem 2 gives an intuitive interpretation to the BOLT loss. It indicates that using BOLT, the model learns to mimic the Bayesian optimal classifier. From the computational point of view, using BOLT leads to gradients that guide the model to approximate the MAP estimator. This finding enables us to use the BOLT loss to train the discriminator of a GAN model. We illustrate this approach in the sequel.

BOLT-GAN Let $s_\theta : \mathcal{X} \rightarrow \mathbb{R}$ denote a model which computes a raw score for input x , and let h_θ be a negative sigmoid activation of its output, i.e.

$$h_\theta(x) = -\sigma(s_\theta(x)). \quad (14)$$

From Theorem 2, one can conclude that in this case, the model h_θ estimates the Bayesian optimal discriminator.

Following a similar approach as in vanilla GAN, we can consider sampling from data and generator distributions conditionally with $P_1 = P_{\text{data}}$ and $P_2 = P_g$ using a prior $\pi = P(\lambda = 1)$ for some $\pi \in (0, 1)$, where $\lambda = 1$ and $\lambda = 2$ correspond to **real** and **fake** samples, respectively. Noting that the generator samples are given by $g_\phi(Z)$ for latent samples $Z \sim P_Z$, the expected BOLT loss of the discriminator is given by

$$R_{\text{BOLT}}(\phi, \theta) = -\mathcal{L}_{\text{BOLT}}(\phi, \theta), \quad (15)$$

with $\mathcal{L}_{\text{BOLT}}(\phi, \theta)$ being

$$\begin{aligned} \mathcal{L}_{\text{BOLT}}(\phi, \theta) &= \pi \mathbb{E}_{X \sim P_{\text{data}}} [h_\theta(X)] \\ &\quad (1 - \pi) \mathbb{E}_{Z \sim P_Z} [h_\theta(g_\phi(Z))]. \end{aligned} \quad (16)$$

Given this risk function, the generator and discriminator are jointly trained by maximizing the minimum loss. This is equivalent to solving the following min-max game:

$$\min_{\phi} \max_{\theta} \mathcal{L}_{\text{BOLT}}(\phi, \theta). \quad (17)$$

Considering Theorem 1, one can see that the inner optimization minimizes the Bayes error upper bound.⁴

Stability of BOLT-GAN The learning objective in BOLT-GAN is similar to that of WGAN, with two main differences: (i) BOLT-GAN considers an arbitrary sampling prior π , as in vanilla GAN, and (ii) it does not impose any Lipschitz continuity restriction on the discriminator model. The discussions in (Arjovsky et al., 2017; Gulrajani et al., 2017; Miyato et al., 2018) suggest that the latter difference can lead to lack of stability, when we use BOLT-GAN in this vanilla form. Our numerical experiments confirm the validity of this conjecture. To understand the reason behind this behavior, we study the convergence of the vanilla BOLT-GAN in the sequel. Our result indicates that BOLT-GAN implicitly minimizes the total variation (TV), which is a strict notion of distance. This finding enables us to modify the BOLT-GAN learning objective to a stable form.

3.2 Convergence of BOLT-GAN

Consider the general learning objective

$$\begin{aligned} \mathcal{L}_{\text{BG}}^{(\pi)}(g, h) &= \pi \mathbb{E}_{X \sim P_{\text{data}}} [h(X)] \\ &\quad - (1 - \pi) \mathbb{E}_{Z \sim P_Z} [h(g(Z))], \end{aligned} \quad (18)$$

which is defined for any measurable $h : \mathcal{X} \mapsto [0, 1]$ and measurable $g : \mathcal{Z} \mapsto \mathcal{X}$ that maps that latent space \mathcal{Z} to the data space. $\mathcal{L}_{\text{BG}}^{(\pi)}$ reduces to $\mathcal{L}_{\text{BOLT}}$, when we replace g and h are parameterized models g_θ and h_θ .

Our goal is to understand the metric, under which the generator distribution P_g converges to P_{data} , when the min-max game with objective $\mathcal{L}_{\text{BG}}^{(\pi)}$ is solved. To this end, let us first define total variation (TV).

Definition 1 (Total variation norm). *The total variation between two distributions P and Q defined on a measurable \mathcal{X} is defined as*

$$TV(P, Q) = \sup_{A \subseteq \mathcal{X}} |P(A) - Q(A)|, \quad (19)$$

with the supremum taken over all events A in the σ -field over \mathcal{X} .

⁴Note that $\mathcal{L}_{\text{BOLT}} = -R_{\text{BOLT}}$.

The convergence of TV to zero implies for convergence of other distances, such as including JS and EM. The following lemma gives an alternative representation for TV.

Lemma 1 (Dudley (2002a)). *The total variation between P and Q is equivalently given by*

$$TV(P, Q) = \sup_{f: \mathcal{X} \rightarrow [0, 1]} \int f d(P - Q), \quad (20)$$

where the difference $P - Q$ is a signed measure on \mathcal{X} .

The following theorem characterizes the connection between the BOLT-GAN learning objective $\mathcal{L}_{BG}^{(\pi)}$ and the TV between the generator and the data distributions.

Theorem 3 (BOLT vs TV). *Fix the prior $\pi \in (0, 1)$. For generator g , let P_g denote the distribution of $g(Z)$, when $Z \sim P_Z$. Define $D^{(\pi)}$ as*

$$D^{(\pi)}(g) \triangleq \max_h \mathcal{L}_{BG}^{(\pi)}(g, h), \quad (21)$$

with the maximum taken over all discriminators, i.e., all $h : \mathcal{X} \mapsto [0, 1]$. Then, $D^{(\pi)}$ satisfies the following property

$$D^{(\pi)}(g) + D^{(1-\pi)}(g) \geq TV(P_{\text{data}}, P_g). \quad (22)$$

with equality when $\pi = 0.5$.

Proof. From the definition (18), we have

$$\begin{aligned} \mathcal{L}_{BG}^{(\pi)}(g, h) + \mathcal{L}_{BG}^{(1-\pi)}(g, h) &= \mathbb{E}_{X \sim P_{\text{data}}}[h(X)] \\ &\quad - \mathbb{E}_{Z \sim P_Z}[h(g(Z))], \end{aligned} \quad (23)$$

which noting that $g(Z)$ is distributed as P_g can be written as

$$\begin{aligned} \mathcal{L}_{BG}^{(\pi)}(g, h) + \mathcal{L}_{BG}^{(1-\pi)}(g, h) &= \mathbb{E}_{X \sim P_{\text{data}}}[h(X)] \\ &\quad - \mathbb{E}_{X \sim P_g}[h(X)]. \end{aligned} \quad (24)$$

Setting the signed metric $P_{\text{data}} - P_g$ to be the difference of densities, we can conclude that

$$\Sigma(g) \triangleq \max_{h: \mathcal{X} \mapsto [0, 1]} [\mathcal{L}_{BG}^{(\pi)}(g, h) + \mathcal{L}_{BG}^{(1-\pi)}(g, h)] \quad (25)$$

$$= \max_{h: \mathcal{X} \mapsto [0, 1]} \left[\int h(X) d(P_{\text{data}} - P_g) \right] \quad (26)$$

$$\stackrel{(a)}{=} TV(P_{\text{data}}, P_g), \quad (27)$$

where (a) follows from Lemma 1. We next use the fact that

$$\Sigma(g) \leq \max_h [\mathcal{L}_{BG}^{(\pi)}(g, h)] + \max_h [\mathcal{L}_{BG}^{(1-\pi)}(g, h)], \quad (28)$$

and using the definition of $D^{(\pi)}$ to conclude that

$$TV(P_{\text{data}}, P_g) = \Sigma(g) \quad (29)$$

$$\leq D^{(\pi)}(g) + D^{(1-\pi)}(g) \quad (30)$$

which proves the inequality. We further note that with $\pi = 0.5$

$$\begin{aligned} TV(P_{\text{data}}, P_g) &= \Sigma(g) \\ &= \max_h [\mathcal{L}_{BG}^{(0.5)}(g, h) + \mathcal{L}_{BG}^{(0.5)}(g, h)] \\ &= 2D^{(0.5)}(g) \end{aligned} \quad (31)$$

which indicates that equality is achieved with $\pi = 0.5$. \square

The above result indicates that using BOLT-GAN, the generator distribution converges to the data distribution at least as strong as minimizing the TV between the two distributions.

Corollary 1 (Half-TV guarantee). *Let $D^{(\pi)}$ be as in Theorem 3. Assume for a given generator g , we have*

$$\max \left\{ D^{(\pi)}(g), D^{(1-\pi)}(g) \right\} \leq \varepsilon \quad (32)$$

Then, the TV between the generator and data distributions is bounded as

$$\text{TV}(P_{\text{data}}, P_g) \leq 2\varepsilon. \quad (33)$$

Proof. Using Theorem 3, we have

$$2 \max \left\{ D^{(\pi)}(g), D^{(1-\pi)}(g) \right\} \geq D^{(\pi)}(g) + D^{(1-\pi)}(g) \quad (34)$$

$$\geq \text{TV}(P_{\text{data}}, P_g). \quad (35)$$

We can hence write

$$\varepsilon \geq \max \left\{ D^{(\pi)}(g), D^{(1-\pi)}(g) \right\} \quad (36)$$

$$\geq \frac{1}{2} \text{TV}(P_{\text{data}}, P_g). \quad (37)$$

which concludes the proof. \square

The above result suggests that the BOLT-GAN objective encourages the generated distribution P_g to approach the true data distribution P_{data} under the total variation (TV) metric.

3.3 Regularized BOLT-GAN via Lipschitz

Lipschitz critics are known to stabilize adversarial training and provide informative, non-saturating gradients Arjovsky et al. (2017); Gulrajani et al. (2017); Miyato et al. (2018). Motivated by this, we enforce 1-Lipschitz constraint on the discriminator. Intuitively, this can lead to better gradients while training the generator. This can reduce gradient explosion or vanishing, as well as the variance of stochastic updates flowing through $\nabla_\phi h_\theta(g_\phi(z))$. In this section, we show that under this modification, the BOLT-GAN implies a *weaker* notion of convergence and better stability.

Lipschitz BOLT-GAN The Lipschitz BOLT-GAN trains the generator and discriminator by solving the min-max game (17), subject to Lipschitz continuity of the discriminator. More precisely, it solves

$$\min_{\phi} \max_{h \in \mathcal{H}_{\text{Lip}}} \mathcal{L}_{\text{BOLT}}(\phi, \theta), \quad (38)$$

where \mathcal{H}_{Lip} is the set of functions $h_\theta : \mathcal{X} \mapsto [-1, 0]$ and

$$\begin{aligned} \mathcal{H}_{\text{Lip}} = \{h : \mathcal{X} \mapsto [0, 1] : & |h(x) - h(y)| \leq \|x - y\| \\ & \forall x, y \in \mathcal{X}\}, \end{aligned} \quad (39)$$

The Lipschitz continuity further imposes a smoothness regularization on the BOLT-GAN discriminator.

For simplicity, we drop the subscript θ in h_θ , stating the following theorem. 4.

Theorem 4 (Convergence of Lipchitz BOLT-GAN). *Fix $0 < \pi \leq 0.5$, and define the bounded 1-Lipschitz class of discriminator models as*

$$\begin{aligned} \mathcal{H}_{\text{Lip}} = \{h : \mathcal{X} \mapsto [0, 1] : & |h(x) - h(y)| \leq \|x - y\| \\ & \forall x, y \in \mathcal{X}\}, \end{aligned} \quad (40)$$

for some norm $\|\cdot\|$ defined on data space \mathcal{X} . For the generator model g , define

$$D_{\text{Lip}}^{(\pi)}(g) \triangleq \max_{h \in \mathcal{H}_{\text{Lip}}} L_{\text{BG}}^{(\pi)}(g, h), \quad (41)$$

with $L_{\text{BG}}^{(\pi)}(g, h)$ being defined in (18). Then, for any prior $0 < \pi \leq 0.5$, we have

$$D_{\text{Lip}}^{(\pi)}(g) \leq W_1(P_{\text{data}}, P_g). \quad (42)$$

where W_1 is the Lipchitz Wasserstein-1 measure defined in (46) below.

Proof. Starting from (24) in the proof of Theorem 3, we can write

$$\Sigma_{\text{Lip}}(g) \triangleq \max_{h \in \mathcal{H}_{\text{Lip}}} \left[\mathcal{L}_{\text{BG}}^{(\pi)}(g, h) + \mathcal{L}_{\text{BG}}^{(1-\pi)}(g, h) \right] \quad (43)$$

$$= \max_{h \in \mathcal{H}_{\text{Lip}}} \left\{ \mathbb{E}_{X \sim P_{\text{data}}} [h(X)] - \mathbb{E}_{X \sim P_g} [h(X)] \right\}. \quad (44)$$

In the supplementary file, we show that for $0 < \pi \leq 0.5$,

$$D_{\text{Lip}}^{(\pi)}(g) \leq \max_{h \in \mathcal{H}_{\text{Lip}}} \left[\mathcal{L}_{\text{BG}}^{(\pi)}(g, h) + \mathcal{L}_{\text{BG}}^{(1-\pi)}(g, h) \right] \quad (45)$$

and therefore

$$D_{\text{Lip}}^{(\pi)}(g) \leq \max_{h \in \mathcal{H}_{\text{Lip}}} \left\{ \mathbb{E}_{X \sim P_{\text{data}}} [h(X)] - \mathbb{E}_{X \sim P_g} [h(X)] \right\}.$$

The Kantorovich-Rubinstein duality (Villani et al., 2009) gives

$$\begin{aligned} W_1(P_{\text{data}}, P_g) &= \\ &\sup_{h \in \mathcal{H}_{\text{Lip}}^+} \left\{ \mathbb{E}_{X \sim P_{\text{data}}} [h(X)] - \mathbb{E}_{X \sim P_g} [h(X)] \right\}, \end{aligned} \quad (46)$$

where $\mathcal{H}_{\text{Lip}}^+$ denotes the set of all 1-Lipschitz functions on \mathcal{X}

$$\mathcal{H}_{\text{Lip}}^+ = \{h : |h(x) - h(y)| \leq \|x - y\| \ \forall x, y \in \mathcal{X}\}. \quad (47)$$

Noting that $\mathcal{H}_{\text{Lip}} \subset \mathcal{H}_{\text{Lip}}^+$, we can write

$$\begin{aligned} W_1(P_{\text{data}}, P_g) &\geq \\ &\sup_{h \in \mathcal{H}_{\text{Lip}}} \left\{ \mathbb{E}_{X \sim P_{\text{data}}} [h(X)] - \mathbb{E}_{X \sim P_g} [h(X)] \right\}, \end{aligned} \quad (48)$$

$$\geq D_{\text{Lip}}^{(\pi)}(g). \quad (49)$$

This concludes the proof. \square

The above result indicates an interesting dichotomy. While the WGAN implicitly minimizes the Earth-Mover (Wasserstein-1) distance between P_{data} and P_g , the BOLT-GAN objective can be viewed as implicitly minimizing the total variation (TV) distance. The Lipschitz BOLT-GAN, on the other hand, bridges these two perspectives by enforcing Lipschitz continuity, thereby promoting a smoother optimization landscape. This intuition may be suggestive of the relative advantages of these three methods.

Lipschitz enforcement. We impose Lipschitzness on h_θ by adding a gradient penalty (GP, $\lambda_{\text{GP}}=10$) (Gulrajani et al., 2017): for $\hat{x} = \epsilon x + (1 - \epsilon)g_\phi(z)$ with $\epsilon \sim \mathcal{U}(0, 1)$, we add $\lambda_{\text{GP}} \mathbb{E}_{\hat{x}} (\|\nabla_{\hat{x}} h_\theta(\hat{x})\|_2 - 1)^2$ to the loss. Alternatives (spectral normalization, weight clipping) and implementation details are discussed in the supplement.

4 Experiments and Results

To establish the benefits of the lipchitz BOLT-GAN design, we conduct experiments on standard image generation tasks using the MNIST (LeCun et al., 1998) dataset. and CelebA (Liu et al., 2015). We use the Fréchet inception distance (FID) (Heusel et al., 2017) to assess the quality of the generated images over training epochs and provide comparisons to the WGAN.

4.1 Experimental Setup

We adopt a residual DCGAN backbone (Gulrajani et al., 2017): the generator upsamples a set of 128-D Gaussian latent images to 64×64 RGB via residual blocks; the critic symmetrically downsamples these images with global-sum pooling and a final linear head for classification. BatchNorm/ReLU activation is used in the generator. LeakyReLU in the critic, with a Lipschitz constraint enforced through a gradient penalty ($\lambda_{GP} = 10$). We evaluate performance on **CIFAR-10**, **CelebA-64**, and **LSUN Bedroom/Church-64**. For training we use Adam ($\alpha = 2 \times 10^{-4}$, $\beta_1 = 0.5$, $\beta_2 = 0.999$), with batch size 64, for 20 epochs. FID (Heusel et al., 2017) is computed every 5 epochs on 10,000 samples using `torch-fidelity` (Seitzer, 2020), averaged over three seeds. Additional architectural and hardware details appear in the supplementary.

4.2 Quantitative and Convergence Results

Table 3 shows that BOLT-GAN consistently surpasses WGAN, achieving 10–60% lower FID across all benchmarks. As illustrated in Figure 1, it also converges faster and exhibits smoother training dynamics with reduced variance and fewer oscillations. Complementary qualitative results in Figure 2 highlight sharper textures and fewer artifacts in samples generated by BOLT-GAN after 100 epochs on CIFAR-10. We also trained BOLT-GAN without Lipschitz regularization. This TV-based variant quickly diverges (FID > 300 –400), confirming that the gradient-penalty term is essential for stability.

Table 1: FID (\downarrow) after 20 epochs for the non-Lipschitz BOLT-GAN ($\lambda_{GP} = 0$) compared with the Lipschitz version.

Dataset	Non-Lipschitz ($\lambda_{GP} = 0$)	Lipschitz ($\lambda_{GP} = 10$)
CIFAR-10	≈ 350 (unstable)	44.2 ± 1.2
CelebA-64	≈ 300	9.2 ± 0.4
LSUN Bedroom-64	Diverged (> 400)	40.3 ± 2.3

4.3 Ablation Studies

Label smoothing in BCE can be mimicked in the non-Lipschitz (TV) BOLT-GAN by using an unbalanced prior ($\pi_{\text{real}}=0.45$, $\pi_{\text{fake}}=0.55$); Table 5 shows a modest 2–3% FID improvement over $\pi_{\text{real}}=0.50$. To test robustness, we sweep $\lambda_{GP} \in \{1, 5, 10, 20\}$ for 20 epochs and report FID averaged over three seeds; performance stays within ± 1 FID across the range (Fig. 3, Tab. 4). Under identical settings, BOLT-GAN-GP consistently attains 10–60 % lower FID than WGAN-GP. Both reach their best stability around $\lambda_{GP} \in [5, 10]$ (Table 2).

Table 2: FID (\downarrow) of WGAN-GP and BOLT-GAN-GP on CIFAR-10 across different values of λ_{GP} .

Method	$\lambda_{GP} = 1$	5	10	20
WGAN-GP	60.8	59.6	60.0	61.1
BOLT-GAN-GP	44.3	43.6	44.2	46.7

5 Conclusion

This paper has presented BOLT-GAN, a streamlined modification of the WGAN framework inspired by the Bayes optimal learning threshold (BOLT). Through extensive experiments on four diverse image-generation

Table 3: FID (\downarrow) after 20 epochs.

Dataset	WGAN	BOLT GAN	Relative Δ (%)
CIFAR-10	60.0 ± 1.8	44.2 ± 1.2	-26.3
CelebA-64	10.3 ± 0.5	9.2 ± 0.4	-10.7
LSUN Bedroom-64	102.5 ± 2.9	40.3 ± 2.3	-60.7
LSUN Church-64	43.5 ± 1.4	14.8 ± 0.6	-65.9

Table 4: Best FID (\downarrow) after 20 epochs for different λ_{GP} . Bold marks the default used in all other experiments.

Dataset	λ_{GP}			
	1	5	10	20
CIFAR-10	44.3 ± 1.2	43.6 ± 1.1	44.2 ± 1.2	46.7 ± 1.3
CelebA-64	10.5 ± 0.5	9.4 ± 0.4	9.2 ± 0.4	10.0 ± 0.5

Table 5: CIFAR-10 FID at 20 ep with balanced vs. imbalanced prior.

Configuration	FID	Δ vs. $\pi = 0.50$
Balanced ($\pi = 0.50$)	44.2	—
Imbalanced ($\pi = 0.45$)	43.1	-2.4%

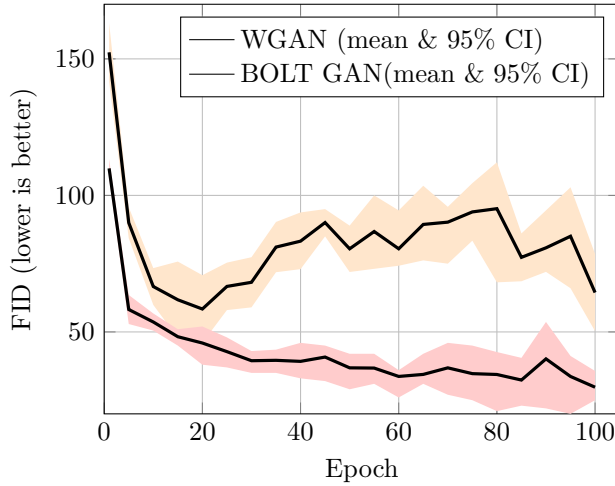
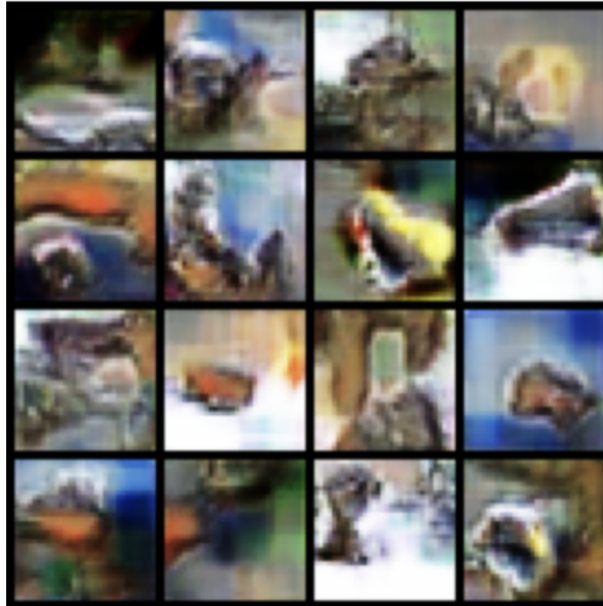
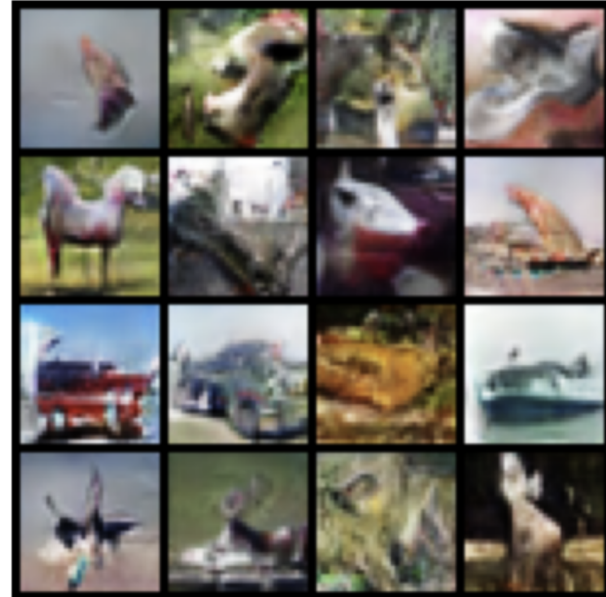


Figure 1: CIFAR-10 FID vs. epochs (mean \pm std, 3 seeds).

benchmarks, namely CIFAR-10, CelebA-64, LSUN Bedroom-64, and LSUN Church-64, we have demonstrated that BOLT-GAN consistently produces smoother training dynamics and lowers FID scores by 10-60% compared to the standard WGAN. These gains hold across both low- and high-resolution settings, underscoring the robustness and generality of our approach. The current study introduces two extreme cases of BOLT-GAN, namely the vanilla and Lipschitz BOLT-GAN. While the former minimizes the total variation, the latter restricts a metric that is weaker than the Wasserstein distance. Exploring constraints under which BOLT-GAN framework restricts alternative measures remains an interesting direction for future research.



(a) WGAN



(b) BOLT-GAN

Figure 2: CIFAR-10 samples at 100 epochs.

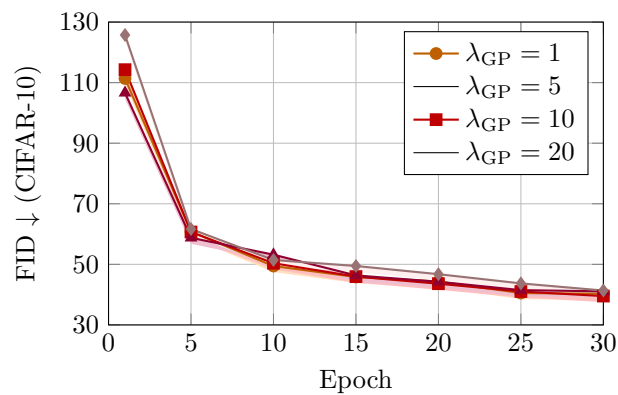


Figure 3: CIFAR-10 FID vs. epochs for different λ_{GP} (mean \pm std, 3 seeds).

References

Anil, C., Lucas, J., and Grosse, R. (2019). Sorting out lipschitz function approximation. In *International Conference on Machine Learning (ICML)*, pages 291–301. PMLR.

Arjovsky, M., Chintala, S., and Bottou, L. (2017). Wasserstein Generative Adversarial Networks. In *International Conference on Machine Learning (ICML)*, pages 214–223. PMLR.

Arora, S., Ge, R., Liang, Y., Ma, T., and Zhang, Y. (2017). Generalization and equilibrium in generative adversarial nets (gans). In *International Conference on Machine Learning (ICML)*, pages 224–232. PMLR.

Berthelot, D., Schumm, T., and Metz, L. (2017). Began: Boundary equilibrium generative adversarial networks. In *arXiv preprint arXiv:1703.10717*.

Bhattacharyya, A. (1943). On a measure of divergence between two statistical populations defined by their probability distributions. *Bulletin of the Calcutta Mathematical Society*, 35:99–109.

Bishop, C. M. (2006). *Pattern recognition and machine learning*. Springer.

Cissé, M., Bojanowski, P., Grave, E., Dauphin, Y., and Usunier, N. (2017). Parseval networks: Improving robustness to adversarial examples. In *International Conference on Machine Learning (ICML)*, pages 854–863. PMLR.

Cybenko, G. (1989). Approximation by superpositions of a sigmoidal function. *Mathematics of Control, Signals and Systems*, 2(4):303–314.

Devroye, L., Györfi, L., and Lugosi, G. (1996). *A Probabilistic Theory of Pattern Recognition*. Springer Science & Business Media.

Dudley, R. M. (2002a). *Real Analysis and Probability*. Cambridge Studies in Advanced Mathematics. Cambridge University Press, 2 edition.

Dudley, R. M. (2002b). *Real Analysis and Probability*. Cambridge University Press.

Fukunaga, K. (2013). *Introduction to Statistical Pattern Recognition*. Academic press.

Goodfellow, I. J., Pouget-Abadie, J., Mirza, M., Xu, B., Warde-Farley, D., Ozair, S., Courville, A., and Bengio, Y. (2014). Generative Adversarial Nets. In *Advances in Neural Information Processing Systems (NeurIPS)*, volume 27.

Gulrajani, I., Ahmed, F., Arjovsky, M., Dumoulin, V., and Courville, A. (2017). Improved training of Wasserstein GANs. In *Advances in Neural Information Processing Systems (NeurIPS)*, volume 30.

Heusel, M., Ramsauer, H., Unterthiner, T., Nessler, B., and Hochreiter, S. (2017). GANs trained by a two time-scale update rule converge to a local nash equilibrium. In *Advances in Neural Information Processing Systems (NeurIPS)*, volume 30.

Karras, T., Aila, T., Laine, S., and Lehtinen, J. (2018). Progressive growing of GANs for improved quality, stability, and variation. In *International Conference on Learning Representations (ICLR)*.

Kodali, N., Abernethy, J., Hays, J., and Kira, Z. (2017). On convergence and stability of gans. In *arXiv preprint arXiv:1705.07215*.

LeCun, Y., Bottou, L., Bengio, Y., and Haffner, P. (1998). Gradient-based learning applied to document recognition. *Proceedings of the IEEE*, 86(11):2278–2324.

Liu, Z., Luo, P., Wang, X., and Tang, X. (2015). Deep learning face attributes in the wild. In *Proceedings of the IEEE International Conference on Computer Vision (ICCV)*, pages 3730–3738.

Lu, J., Shen, Z., Yang, H., and Zhang, S. (2020). Deep network approximation for smooth functions. *SIAM Journal on Mathematical Analysis*, 52(6):5465–5507.

Mahalanobis, P. C. (1936). On the generalized distance in statistics. *Proceedings of the National Institute of Sciences (Calcutta)*, 2:49–55.

Mao, X., Li, Q., Xie, H., Lau, R. Y., Wang, Z., and Smolley, S. P. (2017). Least squares generative adversarial networks. In *Proceedings of the IEEE International Conference on Computer Vision (ICCV)*, pages 2794–2802.

Mescheder, L., Geiger, A., and Nowozin, S. (2018). Which training methods for gans do actually converge? In *International Conference on Machine Learning (ICML)*, pages 3481–3490. PMLR.

Miyato, T., Kataoka, T., Koyama, M., and Yoshida, Y. (2018). Spectral normalization for generative adversarial networks. In *International Conference on Learning Representations (ICLR)*.

Moon, K. R., Sricharan, K., and Hero III, A. O. (2017). Ensemble estimation of distributional functionals via k -nearest neighbors. *arXiv preprint arXiv:1707.03083*.

Naeini, M. T., Bereyhi, A., Noshad, M., Liang, B., and Hero, A. O. (2025). Universal training of neural networks to achieve Bayes Optimal Classification Accuracy. In *IEEE International Conference on Acoustics, Speech and Signal Processing (ICASSP)*, pages 1–5.

Noshad, M., Xu, L., and Hero, A. (2019). Learning to benchmark: Determining best achievable misclassification error from training data. *arXiv preprint arXiv:1909.07192*.

Nowozin, S., Cseke, B., and Tomioka, R. (2016). f-gan: Training generative neural samplers using variational divergence minimization. In *Advances in Neural Information Processing Systems (NeurIPS)*, volume 29.

Petzka, H., Fischer, A., and Lukovnicov, D. (2018). On the regularization of Wasserstein GANs. In *International Conference on Learning Representations (ICLR) Workshop*.

Saatchi, Y. and Wilson, A. G. (2017). Bayesian GAN. In *Advances in Neural Information Processing Systems (NeurIPS)*, volume 30.

Seitzer, M. (2020). Pytorch-fid: FID Score for PyTorch. *GitHub repository*.

Shalev-Shwartz, S. and Ben-David, S. (2014). *Understanding Machine Learning: From Theory to Algorithms*. Cambridge University Press, Cambridge, UK.

Villani, C. et al. (2009). *Optimal Transport: Old and New*, volume 338. Grundlehren der mathematischen Wissenschaften, Springer, Berlin, Germany.

Ye, N. and Zhu, Z. (2018). Bayesian Adversarial Learning. In *Advances in Neural Information Processing Systems (NeurIPS)*, volume 31.

Zhang, C., Bengio, S., Hardt, M., Recht, B., and Vinyals, O. (2021). Understanding deep learning (still) requires rethinking generalization. *Communications of the ACM*, 64(3):107–115.

A Definitions and Preliminaries

A.1 Metrics

We recall the total variation (TV) distance and the Wasserstein- p distance, together with basic equivalences used in our analysis.

Definition 2 (Total variation). *Let P and Q be probability measures on a measurable space $(\mathcal{X}, \mathcal{F})$. The total variation distance is*

$$\text{TV}(P, Q) := \sup_{A \in \mathcal{F}} |P(A) - Q(A)|. \quad (50)$$

The total variation can be computed by equivalent forms. The following lemma gives two equivalent expressions for it.

Lemma 2 (Equivalent forms of total variation (Dudley, 2002b)). *For probability measures P and Q on $(\mathcal{X}, \mathcal{F})$,*

$$\text{TV}(P, Q) = \sup_{f: \mathcal{X} \rightarrow [0, 1]} (\mathbb{E}_{X \sim P}[f(X)] - \mathbb{E}_{X \sim Q}[f(X)]) \quad (51)$$

$$= \frac{1}{2} \sup_{\|g\|_\infty \leq 1} \left| \mathbb{E}_{X \sim P}[g(X)] - \mathbb{E}_{X \sim Q}[g(X)] \right|, \quad (52)$$

and if P and Q are absolutely continuous w.r.t. a σ -finite measure μ with densities P and Q ,

$$\text{TV}(P, Q) = \frac{1}{2} \int_{\mathcal{X}} |p(x) - q(x)| d\mu(x). \quad (53)$$

Next, we define the Wasserstein distance.

Definition 3 (Wasserstein- p distance). *Let (\mathcal{X}, d) be a metric space and $p \in [1, \infty)$. For probability measures P and Q on \mathcal{X} with finite p -th moments, the Wasserstein- p distance is*

$$W_p(P, Q) := \left(\inf_{\gamma \in \Gamma(P, Q)} \int_{\mathcal{X} \times \mathcal{X}} d(x, y)^p d\gamma(x, y) \right)^{1/p}, \quad (54)$$

where $\Gamma(P, Q)$ is the set of couplings with marginals P and Q .

The Kantorovich–Rubinstein duality result gives an alternative expression for the Wasserstein-1 distance.

Definition 4 (Lipschitz continuity). *A function $f: (\mathcal{X}, \|\cdot\|) \rightarrow \mathbb{R}$ is said to be L -Lipschitz if*

$$|f(x) - f(y)| \leq L \|x - y\| \quad \forall x, y \in \mathcal{X}.$$

Its global Lipschitz constant is denoted

$$\text{Lip}(f) := \sup_{x \neq y} \frac{|f(x) - f(y)|}{\|x - y\|}.$$

Hence $\text{Lip}(f) \leq 1$ exactly when f is 1-Lipschitz.

Lemma 3 (Kantorovich–Rubinstein duality for W_1 (Villani et al., 2009)). *On a Polish metric space (\mathcal{X}, d) , for probability measures P, Q with finite first moments,*

$$W_1(P, Q) = \sup_{\text{Lip}(f) \leq 1} (\mathbb{E}_{X \sim P}[f(X)] - \mathbb{E}_{Y \sim Q}[f(Y)]), \quad (55)$$

where $\text{Lip}(f) \leq 1$ means $|f(x) - f(y)| \leq d(x, y)$ for all $x, y \in \mathcal{X}$.

In general, the total variation is a stronger notion of distance in the probability space. This can be observed from the following result.

Lemma 4 (Bounding W_1 by TV on bounded spaces (Villani et al., 2009)). *If (\mathcal{X}, d) has finite diameter $D := \sup_{x,y} d(x, y) < \infty$, then for all probability measures P and Q ,*

$$W_1(P, Q) \leq D \text{TV}(P, Q). \quad (56)$$

Sketch. By Lemma 3, scale any 1-Lipschitz f to $\tilde{f} \in [0, D]$ and apply (51).

A.2 BOLT and BOLT-GAN

Throughout, we use the following functional objectives. These objectives match the definitions given in the main paper (see Sec. 3).

Definition 5 (BOLT functional). *For a measurable $h : \mathcal{X} \rightarrow [-1, 0]$,*

$$\mathcal{L}_{\text{BOLT}}(h) = q_2 - \left(q_1 \mathbb{E}_{X \sim P_1}[h(X)] - q_2 \mathbb{E}_{X \sim P_2}[h(X)] \right). \quad (57)$$

The universal bound of Naeini et al. (2025, Thm. 1) implies that for any such h , $\varepsilon_{\text{Bayes}} \leq \mathcal{L}_{\text{BOLT}}(h)$.

Risk and per-example BOLT loss Let $Y \in \{1, 2\}$, $X \mid (Y = i) \sim P_i$, and let $h : \mathcal{X} \rightarrow [-1, 0]$ be measurable. Define $s(y) := \mathbb{1}\{y = 2\} - \mathbb{1}\{y = 1\} \in \{-1, +1\}$ (or equivalently, $s(y) = (-1)^y$). We further define the per-example BOLT loss and the population risk:

$$\ell_{\text{BOLT}}(z, y) := s(y) z, \quad (58)$$

$$R(h) := \mathbb{E}[\ell_{\text{BOLT}}(h(X), Y)] = -q_1 \mathbb{E}_{X \sim P_1}[h(X)] + q_2 \mathbb{E}_{X \sim P_2}[h(X)]. \quad (59)$$

With the BOLT functional from Def. 5,

$$\mathcal{L}_{\text{BOLT}}(h) = q_2 - \left(q_1 \mathbb{E}_{X \sim P_1}[h(X)] - q_2 \mathbb{E}_{X \sim P_2}[h(X)] \right) \quad (60)$$

$$= q_2 + R(h), \quad (61)$$

so the minimizers of $R(h)$ coincide with the minimizers of $\mathcal{L}_{\text{BOLT}}(h)$.

Definition 6 (Prior-weighted GAN/BOLT-GAN functional). *Let g be a generator inducing P_g , and let $h : \mathcal{X} \rightarrow [0, 1]$ be a bounded critic. For prior $\pi \in (0, 1)$,*

$$\mathcal{L}_{\text{BG}}^{(\pi)}(g, h) := \pi \mathbb{E}_{X \sim P_{\text{data}}}[h(X)] - (1 - \pi) \mathbb{E}_{X \sim P_g}[h(X)]. \quad (62)$$

It is worth mentioning that $\mathcal{L}_{\text{BG}}^{(\pi)}(g, h)$ satisfies the complementary-sum identity

$$\mathcal{L}_{\text{BG}}^{(\pi)}(g, h) + \mathcal{L}_{\text{BG}}^{(1-\pi)}(g, h) = \mathbb{E}_{X \sim P_{\text{data}}}[h(X)] - \mathbb{E}_{X \sim P_g}[h(X)]. \quad (63)$$

This is used repeatedly in our analysis to connect the BOLT-GAN objective to the TV and Wasserstein distance (see Secs. 3.2–3.3 of the main paper).

B Proofs and Further Results on BOLT

In this section we restate the result on the BOLT-assisted estimator of MAP classifier given in the main paper and provide a complete proof.

Theorem 5 (BOLT Estimator of MAP Classifier (Theorem 2 from main paper)). *Let (X, Y) describe a binary classification problem with $Y \in \{1, 2\}$, priors $q_1 = \Pr\{Y = 1\}$ and $q_2 = \Pr\{Y = 2\}$, class-conditional laws P_1 and P_2 , and posterior*

$$\eta(x) := \Pr\{Y = 1 \mid X = x\}. \quad (64)$$

Let $h^* \in \arg \min_{h: \mathcal{X} \rightarrow [-1,0]} \mathcal{L}_{\text{BOLT}}(h)$ (or equivalently, $h^* \in \arg \min R(h)$). Then, h^* is pointwise optimal almost surely and takes only the endpoint values:

$$h^*(x) = \begin{cases} 0, & \eta(x) > \frac{1}{2}, \\ -1, & \eta(x) < \frac{1}{2}, \\ \text{any } z \in [-1,0], & \eta(x) = \frac{1}{2}. \end{cases} \quad (65)$$

Consequently, the plug-in classifier at threshold -0.5 , i.e.

$$\hat{C}(x) = 1\{h^*(x) \geq -0.5\}, \quad (66)$$

coincides almost everywhere with the MAP decision rule $C_{\text{MAP}}(x) = 1\{\eta(x) \geq \frac{1}{2}\}$. Moreover, if a model h_θ satisfies $\|h_\theta - h^*\|_\infty \leq \epsilon$, then the plug-in decision

$$\hat{C}_\theta(x) = \begin{cases} C_1, & h_\theta(x) \geq -0.5, \\ C_2, & h_\theta(x) < -0.5, \end{cases} \quad (67)$$

is a plug-in estimator of the MAP classifier.

Proof. Fix $x \in \mathcal{X}$ and abbreviate $\eta = \eta(x)$. The conditional risk of predicting a value $z \in [-1,0]$ is

$$r_\eta(z) := \mathbb{E}[\ell_{\text{BOLT}}(z, Y) \mid X = x] \quad (68)$$

$$= \eta \ell_{\text{BOLT}}(z, 1) + (1 - \eta) \ell_{\text{BOLT}}(z, 2) = \quad (69)$$

$$\eta(-z) + (1 - \eta)z = (1 - 2\eta)z. \quad (70)$$

To minimize $r_\eta(z)$ over $z \in [-1,0]$, we can say

1. If $\eta > \frac{1}{2}$, then $1 - 2\eta < 0$. Thus, $r_\eta(z)$ is strictly decreasing in z . The minimum over $[-1,0]$ in this case is attained at the maximal $z = 0$.
2. If $\eta < \frac{1}{2}$, then $1 - 2\eta > 0$. Thus, $r_\eta(z)$ is strictly increasing in z . The minimum therefore occurs at the minimal $z = -1$.
3. If $\eta = \frac{1}{2}$, then $r_\eta(z) \equiv 0$ on $[-1,0]$, and hence any $z \in [-1,0]$ is optimal.

This yields the pointwise characterization (65). Since $\hat{C}(x) = 1\{h^*(x) \geq -0.5\}$ equals $1\{\eta(x) \geq \frac{1}{2}\}$ by (65), the plug-in rule (66) coincides with MAP almost everywhere. The final claim for h_θ follows the fact that $\|h_\theta - h^*\|_\infty \leq \epsilon$ leaves the decision boundary at -0.5 unchanged whenever $h^* \in \{-1,0\}$. \square

Remark 4 (Alternative normalization). If one parametrizes $h : \mathcal{X} \rightarrow [0,1]$ (e.g., the bounded score after sigmoid activation), the same argument applied to the loss $\hat{\ell}(z, y) = (-1)^y(2z-1)$ yields $h^*(x) = 1\{\eta(x) > \frac{1}{2}\}$ and a threshold at $+0.5$. The two normalizations are related by an affine map, which adjusts the threshold accordingly.

Corollary 2 (Bayes consistency of the plug-in classifier). Assume $\Pr(\eta(X) = \frac{1}{2}) = 0$ under the data distribution of (X, Y) . Let $\hat{h}_n : \mathcal{X} \rightarrow [-1,0]$ be risk consistent for ℓ_{BOLT} , i.e.

$$R(\hat{h}_n) \xrightarrow[n \rightarrow \infty]{} \inf_h R(h) = R(h^*), \quad (71)$$

with R as in (59). Define $\hat{C}_n(x) = 1\{\hat{h}_n(x) \geq -0.5\}$. Then the 0-1 risk converges to the Bayes risk:

$$\Pr(\hat{C}_n(X) \neq Y) \xrightarrow[n \rightarrow \infty]{} \Pr(C_{\text{MAP}}(X) \neq Y). \quad (72)$$

Proof. Write the conditional excess risk at x as

$$r_{\eta(x)}(\hat{h}_n(x)) - r_{\eta(x)}(h^*(x)) = |1 - 2\eta(x)| \cdot |\hat{h}_n(x) - h^*(x)|. \quad (73)$$

Then, by (71), we can write

$$R(\hat{h}_n) - R(h^*) = \mathbb{E}[|1 - 2\eta(X)| |\hat{h}_n(X) - h^*(X)|] \rightarrow 0. \quad (74)$$

Fix any $\delta \in (0, 1)$ and split the misclassification event as follows:

$$\mathcal{E}_n := \{\hat{C}_n(X) \neq C_{\text{MAP}}(X)\} = (\mathcal{E}_n \cap \{|1 - 2\eta(X)| \geq \delta\}) \cup \{|1 - 2\eta(X)| < \delta\}. \quad (75)$$

For the case $|1 - 2\eta(X)| \geq \delta$, a decision mismatch implies $|\hat{h}_n(X) - h^*(X)| \geq \frac{1}{2}$ because $h^* \in \{-1, 0\}$ and the plug-in threshold is -0.5 . Therefore,

$$R(\hat{h}_n) - R(h^*) \geq \mathbb{E}[|1 - 2\eta(X)|^{\frac{1}{2}} \mathbf{1}_{\mathcal{E}_n \cap \{|1 - 2\eta(X)| \geq \delta\}}] \quad (76)$$

$$\geq \frac{\delta}{2} \Pr(\mathcal{E}_n \cap \{|1 - 2\eta(X)| \geq \delta\}). \quad (77)$$

Letting $n \rightarrow \infty$ gives $\Pr(\mathcal{E}_n \cap \{|1 - 2\eta(X)| \geq \delta\}) \rightarrow 0$. Moreover, by assumption, $\Pr(|1 - 2\eta(X)| < \delta) \rightarrow 0$ as $\delta \downarrow 0$. We hence first send $n \rightarrow \infty$, and then $\delta \downarrow 0$ in (75) to obtain (72). \square

B.1 Bias and Variance of BOLT

This subsection provides the full statements and proofs corresponding to **Remark 3** in the main paper. We analyze the BOLT loss via plug-in estimators of the likelihood ratio together with a hinge map. The key structural fact is that the population optimizer of the BOLT bound is a hinge of the likelihood ratio; hence optimizing $h(\cdot)$ amounts to estimating $U(x)$, and errors in h mirror errors in U .

Setup and Notation Let (X, C) be binary with classes $C \in \{C_1, C_2\}$, priors $q_i = \Pr\{C = C_i\} > 0$ with $q_1 + q_2 = 1$, and conditionals $X \mid (C = C_i) \sim P_i$ (densities p_i). Define the likelihood ratio $U(x)$ and the prior threshold τ as

$$U(x) := \frac{p_1(x)}{p_2(x)}, \quad \tau := \frac{q_2}{q_1}. \quad (78)$$

Theorem 6 (Optimal bounding function and tightness). *Let $c(x) := q_1 p_1(x) - q_2 p_2(x)$. A pointwise maximizer of $c(x)h(x)$ over $h(x) \in [-1, 0]$ is*

$$h^*(x) = \begin{cases} -1, & U(x) < \tau, \\ 0, & U(x) \geq \tau, \end{cases} \quad (79)$$

and $\mathcal{L}_{\text{BOLT}}(h^*) = \varepsilon_{\text{Bayes}}$.

Proof. We start by showing the endpoint optimality. For fixed x , the map $h \mapsto c(x)h$ is affine on $[-1, 0]$, hence maximized at an endpoint chosen by the sign of $c(x)$, i.e., $h^*(x) = -1$ if $c(x) < 0$ and $h^*(x) = 0$ otherwise. Since $c(x) < 0$ holds if and only if $U(x) < \tau$, we can conclude (79).

We next show the tightness of the result. Using the definition of $\mathcal{L}_{\text{BOLT}}$ (Def. 5, Sec. S1) and substituting h^* , we have

$$\mathcal{L}_{\text{BOLT}}(h^*) = q_2 - \left(q_1 \mathbb{E}_{X \sim P_1}[h^*(X)] - q_2 \mathbb{E}_{X \sim P_2}[h^*(X)] \right) \quad (80)$$

$$= q_2 - \int (q_1 p_1(x) - q_2 p_2(x)) h^*(x) dx \quad (81)$$

$$= q_2 - \int (q_2 p_2(x) - q_1 p_1(x)) \mathbf{1}\{U(x) < \tau\} dx \quad (82)$$

$$= q_2 - \int [q_2 p_2(x) - q_1 p_1(x)]_+ dx \quad (83)$$

$$= 1 - \int \max\{q_1 p_1(x), q_2 p_2(x)\} dx = \varepsilon_{\text{Bayes}}. \quad (84)$$

Here, we have used the fact that $a 1\{a > 0\} = [a]_+$ and $q_2 = \int q_2 p_2$. This completes the proof. \square

The above result gives an interesting connection between the Bayes error and the likelihood ratio.

Corollary 3 (Bayes error as a hinge of likelihood ratio). *With h^* in (79), define the hinge map as*

$$t_0(u) := [q_2 - q_1 u]_+. \quad (85)$$

The Bayes error rate is then given by

$$\varepsilon_{\text{Bayes}} = q_2 - \mathbb{E}_{X \sim P_2}[t_0(U(X))]. \quad (86)$$

Proof. Starting from (81) and using $h^* = -1\{U < \tau\}$,

$$q_1 \mathbb{E}_{P_1}[h^*] - q_2 \mathbb{E}_{P_2}[h^*] = \int (q_1 p_1 - q_2 p_2) h^* dx = \int (q_2 p_2 - q_1 p_1) 1\{U < \tau\} dx \stackrel{\text{label eq : S3 - swap}}{=} \int (q_2 p_2 - q_1 p_1) dx = \mathbb{E}_{X \sim P_2}[q_2 - q_1 U(X)], \quad (87)$$

$$= \int [q_2 p_2 - q_1 p_1]_+ dx = \mathbb{E}_{X \sim P_2}[q_2 - q_1 U(X)]_+, \quad (88)$$

where the last equality is obtain from dividing by $p_2(x)$ on $\{p_2 > 0\}$ (the complement contributes 0). Plugging into the expression for $\mathcal{L}_{\text{BOLT}}(h^*)$, we obtain (86). \square

Plug-in estimator (empirical context). Suppose we observe M_1 samples from class C_1 and M_2 from class C_2 (with total $M = M_1 + M_2$), and set empirical priors $\hat{q}_i := M_i/M$. Let \hat{U} estimate U , and let $X_1^{(2)}, \dots, X_{M_2}^{(2)} \stackrel{\text{i.i.d.}}{\sim} P_2$ be the M_2 samples of class- C_2 used to estimate the expectation over P_2 in (86). Define

$$\hat{t}_0(u) := [\hat{q}_2 - \hat{q}_1 u]_+, \quad \hat{\varepsilon}_{\text{BOLT}} := \hat{q}_2 - \frac{1}{M_2} \sum_{i=1}^{M_2} \hat{t}_0(\hat{U}(X_i^{(2)})). \quad (89)$$

Note $0 \leq t_0(u) \leq q_2 \leq 1$ and $0 \leq \hat{t}_0(u) \leq \hat{q}_2 \leq 1$, so all summands are bounded in $[0, 1]$.

Lemma 5 (Lipschitz property of the hinge). *The map $t_0(u) = [q_2 - q_1 u]_+$ is globally q_1 -Lipschitz:*

$$|t_0(u) - t_0(v)| \leq q_1 |u - v| \quad \forall u, v \in \mathbb{R}. \quad (90)$$

Proof. Let $\tau = q_2/q_1$. If $u, v \leq \tau$, then t_0 is affine with slope $-q_1$, giving equality in (90). If $u, v \geq \tau$, both values are 0. If $u \leq \tau \leq v$ (or vice versa), then $t_0(u) - t_0(v) = t_0(u) = q_2 - q_1 u \leq q_1(\tau - u) \leq q_1|u - v|$. \square

Theorem 7 (Bias and variance of the binary BOLT plug-in estimator). *Assume i.i.d. draws and bounded outputs in $[0, 1]$. Then*

$$|\mathbb{E}[\hat{\varepsilon}_{\text{BOLT}}] - \varepsilon_{\text{Bayes}}| \leq q_1 \mathbb{E}[|\hat{U}(X) - U(X)|] + O(M^{-1/2}), \quad (91)$$

$$\text{Var}(\hat{\varepsilon}_{\text{BOLT}}) = O(M^{-1}). \quad (92)$$

In particular, if $\mathbb{E}[|\hat{U}(X) - U(X)|] \leq \varepsilon_0$, then

$$|\mathbb{E}[\hat{\varepsilon}_{\text{BOLT}}] - \varepsilon_{\text{Bayes}}| \leq q_1 \varepsilon_0 + O(M^{-1/2}). \quad (93)$$

Proof. Bias. By (86)-(89) and adding and subtracting $\mathbb{E}_{X \sim P_2}[t_0(\hat{U}(X))]$, we have:

$$\mathbb{E}[\hat{\varepsilon}_{\text{BOLT}}] - \varepsilon_{\text{Bayes}} = \underbrace{\mathbb{E}_{X \sim P_2}[t_0(U(X)) - t_0(\hat{U}(X))]}_{\text{plug-in error}} + \underbrace{\mathbb{E}[t_0(\hat{U}(X)) - \frac{1}{M_2} \sum_{i=1}^{M_2} \hat{t}_0(\hat{U}(X_i))]}_{\text{sampling/priors}}. \quad (94)$$

By Lemma 5, t_0 is q_1 -Lipschitz, so $|\mathbb{E}_{P_2}[t_0(U) - t_0(\widehat{U})]| \leq q_1 \mathbb{E}_{P_2}[|\widehat{U} - U|]$. For the sampling term, write $Z_i = \widehat{t}_0(\widehat{U}(X_i)) \in [0, 1]$; Hoeffding gives $\mathbb{E}|\frac{1}{M_2} \sum Z_i - \mathbb{E}Z_1| = O(M_2^{-1/2})$. The empirical priors $\widehat{q}_i = M_i/M$ add a zero-mean fluctuation with variance $O(M^{-1})$, hence $O(M^{-1/2})$ in expectation. With fixed class proportions ($M_2 = \Theta(M)$), these contributions are of the same order, yielding (91).

Variance. Using $\widehat{\varepsilon}_{\text{BOLT}} = \widehat{q}_2 - \frac{1}{M_2} \sum_{i=1}^{M_2} Z_i$ with bounded Z_i , $\text{Var}(\frac{1}{M_2} \sum_i Z_i) = O(M_2^{-1})$ and $\text{Var}(\widehat{q}_2) = O(M^{-1})$. Any covariance between these two bounded averages is $O(M^{-1})$ and is dominated by the same order; hence (92). \square

Remark 5 (Typical rates for ε_0). *We bundle approximation and estimation errors into $\varepsilon_0 := \varepsilon_{\text{approx}} + \varepsilon_{\text{est}}$. Under standard smoothness/capacity assumptions,*

$$\varepsilon_0 = O(W^{-\gamma} + N^{-1/2}),$$

where W is a width/capacity proxy, N is the number of training samples used to learn \widehat{U} , and $\gamma > 0$ depends on the target smoothness and the approximating family (Lu et al., 2020; Shalev-Shwartz and Ben-David, 2014).

C Further Results on BOLT-GAN

We present additional properties of the BOLT-GAN objective and its connections to standard distances. Throughout, we use the prior-weighted functional $L_{\text{BG}}^{(\pi)}(g, h)$ as defined in the main text (Sec. 3). We do *not* restate it here to avoid duplication.

Basic bounds. We first preclude degenerate values when the critic is bounded.

Lemma 6 (Lower and upper bounds). *For any generator g and any bounded critic $h : \mathcal{X} \rightarrow [0, 1]$,*

$$\pi - 1 \leq L_{\text{BG}}^{(\pi)}(g, h) \leq \pi. \quad (95)$$

Both bounds are tight in the sense that there exists a pair (g, h) attaining them.

Proof. Since $0 \leq \mathbb{E}_{P_{\text{data}}}[h] \leq 1$ and $0 \leq \mathbb{E}_{P_g}[h] \leq 1$, $L_{\text{BG}}^{(\pi)}(g, h) = \pi \mathbb{E}_{P_{\text{data}}}[h] - (1 - \pi) \mathbb{E}_{P_g}[h] \in [\pi - 1, \pi]$. Tightness follows by choosing distributions and a measurable h that separate supports: if $h = 1$ on $\text{supp}(P_{\text{data}})$ and $h = 0$ on $\text{supp}(P_g)$, the value is π ; if $h = 0$ on $\text{supp}(P_{\text{data}})$ and $h = 1$ on $\text{supp}(P_g)$, it is $\pi - 1$. \square

Monotonicity in the prior. We next show that the maximized gap grows with π .

Lemma 7 (Monotonicity in π). *Fix a generator g with density q and write p for the data density w.r.t. a common dominating measure. Let*

$$D^{(\pi)}(g) := \max_{h: \mathcal{X} \rightarrow [0, 1]} L_{\text{BG}}^{(\pi)}(g, h) = \int_{\mathcal{X}} [\pi p(x) - (1 - \pi) q(x)]_+ dx. \quad (96)$$

Then $D^{(\pi)}(g)$ is nondecreasing in $\pi \in [0, 1]$.

Proof. For each fixed x , the map $\pi \mapsto [\pi p(x) - (1 - \pi) q(x)]_+$ is nondecreasing: its derivative is $p(x) + q(x) > 0$ wherever the bracket is positive and 0 elsewhere. We obtain the desired result by integrating over \mathcal{X} . \square

Balanced vs. prior-weighted gap (Lipschitz critics). We now relate the prior-weighted objective to its “balanced” counterpart on a 1-Lipschitz class. Let:

$$\mathcal{H}_{\text{Lip}} := \{ h : \mathcal{X} \rightarrow [0, 1] : |h(x) - h(y)| \leq \|x - y\| \forall x, y \in \mathcal{X} \}, \quad (97)$$

$$D_{\text{Lip}}^{(\pi)}(g) := \sup_{h \in \mathcal{H}_{\text{Lip}}} \mathbb{E}_{X \sim P_{\text{data}}} [h(X)] - (1 - \pi) \mathbb{E}_{X \sim P_g} [h(X)], \quad (98)$$

$$\Sigma_{\text{Lip}}(g) := \sup_{h \in \mathcal{H}_{\text{Lip}}} \left(\mathbb{E}_{X \sim P_{\text{data}}} [h(X)] - \mathbb{E}_{X \sim P_g} [h(X)] \right). \quad (99)$$

The next inequality is the pointwise scalar comparison we use repeatedly.

Lemma 8 (Pointwise dominance). *For $0 < \pi \leq \frac{1}{2}$ and any $a, b \in [0, 1]$,*

$$\max\{a - b, b - a\} \geq \pi a - (1 - \pi) b. \quad (100)$$

Proof. If $a \geq b$, then

$$(a - b) - (\pi a - (1 - \pi) b) = (1 - \pi)a - \pi b \geq (1 - \pi)b - \pi b = (1 - 2\pi)b \geq 0.$$

If $a < b$, the claim is equivalent to

$$(b - a) - (\pi a - (1 - \pi) b) = (2 - \pi)b - (1 + \pi)a \geq 0,$$

which holds since $a \leq b$ and $(2 - \pi)/(1 + \pi) \geq 1$ for $\pi \leq \frac{1}{2}$. \square

Proposition 1 (From pointwise to functional dominance). *For $0 < \pi \leq \frac{1}{2}$,*

$$D_{\text{Lip}}^{(\pi)}(g) \leq \Sigma_{\text{Lip}}(g). \quad (101)$$

Proof. For any $h \in \mathcal{H}_{\text{Lip}}$, write $a = \mathbb{E}_{P_{\text{data}}} [h]$ and $b = \mathbb{E}_{P_g} [h]$. By Lemma 8, $\max\{a - b, b - a\} \geq \pi a - (1 - \pi) b$. Since $h \mapsto 1 - h$ preserves \mathcal{H}_{Lip} and flips $a - b$ to $b - a$,

$$\sup_{h \in \mathcal{H}_{\text{Lip}}} \max\{a - b, b - a\} = \sup_{h \in \mathcal{H}_{\text{Lip}}} (a - b) = \Sigma_{\text{Lip}}(g).$$

Taking suprema on both sides over $h \in \mathcal{H}_{\text{Lip}}$ yields the claim. \square

Bridge to W_1 (pointer). Combining Proposition 1 with the complementary-sum identity from the main paper and the Kantorovich–Rubinstein dual (sup over all 1-Lipschitz functions without range constraints) gives the bound $D_{\text{Lip}}^{(\pi)}(g) \leq W_1(P_{\text{data}}, P_g)$ used in the main text. We omit the re-statement here to avoid duplication.

Role of the basic bound (Lemma 6). Together with the balanced-sum identity in the paper (Sec. 3), Lemma 6 ensures that each prior-weighted term is uniformly bounded when $h \in [0, 1]$, preventing pathological cancellations when one passes to the balanced form in intermediate maximizations.

Symmetry for $\pi > \frac{1}{2}$. The case $\pi > \frac{1}{2}$ follows by exchanging labels (replacing π with $1 - \pi$, i.e., swapping P_{data} and P_g). Thus the conclusions above extend to all $\pi \in (0, 1]$ by symmetry.

In summary, for $0 < \pi \leq 1$,

$$D_{\text{Lip}}^{(\pi)}(g) \leq \Sigma_{\text{Lip}}(g) \leq W_1(P_{\text{data}}, P_g),$$

This is precisely the inequality chain invoked in the proof of the Lipschitz BOLT–GAN result in the main paper.

D Implementation of Lipschitz BOLT-GAN

This section records the implementation details for our Lipschitz BOLT-GAN experiments. We explain the properties we rely on and the techniques used to enforce the 1-Lipschitz constraint on the discriminator (critic). As discussed in the main paper, Lipschitz continuity is key both (i) to recover meaningful dual objectives (e.g., the KR dual for W_1) and (ii) to stabilize adversarial training; see the TV/Wasserstein connections in Secs. 3.2–3.3. In our code, the gradient penalty is applied to the *raw* critic output \tilde{h}_θ (pre-activation), and the bounded score $h_\theta = \sigma(\tilde{h}_\theta) \in [0, 1]$ is used inside the BOLT objective, as summarized in Algorithm 1. (Gulrajani et al., 2017; Miyato et al., 2018, Sec. 3).

D.1 Preliminaries on Lipschitz continuity

Lemma 9 (Basic Lipschitz calculus (Miyato et al., 2018)). *Let f, g, f_1 , and f_2 be Lipschitz. Then*

$$\text{Lip}(g \circ f) \leq \text{Lip}(g) \text{Lip}(f), \quad (102)$$

$$\text{Lip}(f_1 + f_2) \leq \text{Lip}(f_1) + \text{Lip}(f_2). \quad (103)$$

Lemma 10 (Layerwise Lipschitz constants in common architectures (Miyato et al., 2018; Anil et al., 2019)). *Assume all vector spaces are equipped with the Euclidean norm $\|\cdot\|_2$, and for a function f we write $\text{Lip}(f)$ for its global Lipschitz constant with respect to $\|\cdot\|_2$.*

(i) **Linear / convolutional layers.** *For an affine map $T(x) = Wx + b$ (fully connected) or a convolutional layer viewed as a linear map $x \mapsto Wx$,*

$$\text{Lip}(T) = \|W\|_2,$$

i.e., the operator (spectral) norm of W . Biases do not affect Lip .

(ii) **Pointwise activations (elementwise maps).** *If ϕ is applied elementwise, then $\text{Lip}(\phi) = \sup_{t \in \mathbb{R}} |\phi'(t)|$ (when the derivative exists a.e.).*

(iii) **Residual blocks.** *For a residual block of the form $x \mapsto Sx + F(x)$ with a linear skip S (identity or 1×1 projection),*

$$\text{Lip}(x \mapsto Sx + F(x)) \leq \|S\|_2 + \text{Lip}(F).$$

In particular, if $S = I$, then $\text{Lip} \leq 1 + \text{Lip}(F)$.

(iv) **Resampling operators.** *If S is a (linear) down/up-sampling operator used before or after a block F , then*

$$\text{Lip}(F \circ S) \leq \text{Lip}(F) \|S\|_2, \quad \text{Lip}(S \circ F) \leq \|S\|_2 \text{Lip}(F).$$

Common strided convolutions, pooling, and interpolation are linear maps with finite $\|S\|_2$ that must be accounted for in per-layer bounds.

Remark 6 (Standard elementwise activations and their Lip). *The following are explicit formulas for common activations used in (ii), together with their Lipschitz constants:*

$$\text{ReLU}(t) = \max\{0, t\}, \quad \text{Lip} = 1; \quad \tanh(t) = \frac{e^t - e^{-t}}{e^t + e^{-t}}, \quad \text{Lip} = 1;$$

$$\text{LeakyReLU}_\alpha(t) = \begin{cases} t, & t \geq 0 \\ \alpha t, & t < 0 \end{cases}, \quad \text{Lip} = \max\{1, \alpha\}; \quad \sigma(t) = \frac{1}{1 + e^{-t}}, \quad \sigma'(t) = \sigma(t)(1 - \sigma(t)) \leq \frac{1}{4}, \quad \text{Lip} = \frac{1}{4}.$$

D.2 Spectral Normalization (SN)

Method. Each linear layer W is rescaled by an estimate of its top singular value $\sigma(W)$ via power iteration with persistent vectors (u, v) : $\tilde{W} \leftarrow W/\sigma(W)$. For convolutions, $\sigma(W)$ is the operator norm of the induced linear map and can be estimated by alternating conv/transpose-conv passes. (Miyato et al., 2018).

Guarantee. If every linear/convolutional layer is normalized so that $\|W\|_2 \leq 1$ and all activations are 1-Lipschitz, then by Lemmas 9–10 the whole network is 1-Lipschitz (up to residual additions; see “Residual blocks” below). This yields strong stability at low computational cost and is widely adopted in GAN critics. (Miyato et al., 2018).

Residual blocks and skips. Because $\text{Lip}(x + F(x)) \leq 1 + \text{Lip}(F)$, residual connections can increase the global constant above 1. Two common remedies are: (i) apply SN to the skip 1×1 projection; (ii) scale residual branches by $c < 1$ (“residual scaling”) to keep $\text{Lip}(F) \leq c$, so the block is $\leq 1 + c$.

D.3 Gradient Penalty (GP)

Method. Gradient penalty encourages $\|\nabla_x \tilde{h}_\theta(x)\|_2 \approx 1$ on a chosen sampling distribution. The most common choice is the *interpolation penalty* (Gulrajani et al., 2017): draw $(x_{\text{real}}, x_{\text{fake}})$, form $\hat{x} = \alpha x_{\text{real}} + (1 - \alpha)x_{\text{fake}}$ with $\alpha \sim \text{Unif}[0, 1]$, and add

$$\lambda \mathbb{E}_{\hat{x}} (\|\nabla_{\hat{x}} \tilde{h}_\theta(\hat{x})\|_2 - 1)^2 \quad (104)$$

to the critic loss. We penalize *pre-activation* \tilde{h}_θ , not $\sigma(\tilde{h}_\theta)$, to avoid shrinking gradients through the 1/4-Lipschitz sigmoid.

Guarantee (local, not global). The penalty (104) is a *soft* constraint: it is zero iff the gradient norm equals 1 on the support where it is evaluated (here, segments between real/fake samples). It does not by itself prove a *global* 1-Lipschitz bound, but it aligns with the KR optimal-critic condition and markedly improves training stability. (Gulrajani et al., 2017).

Implementation notes.

- *Backprop through the norm.* Ensure gradients flow through $\|\nabla_{\hat{x}} \tilde{h}_\theta(\hat{x})\|_2$ (autodiff: create graph for higher-order grads).
- *Normalization.* Avoid BatchNorm in the critic; prefer layer/instance norm or none.
- *Lazy regularization.* Apply the penalty every k steps and scale $\lambda \leftarrow k\lambda$ to keep the expected contribution unchanged.
- *Tuning λ .* Start with $\lambda \in [1, 10]$ and monitor the penalty/critic ratio (see diagnostics below).

D.4 Weight clipping

Method. Clip each parameter after every update: $w \leftarrow \text{clip}(w, -L_{\text{wc}}, L_{\text{wc}})$ (Arjovsky et al., 2017). This loosely bounds per-layer operator norms via element-wise bounds.

Guarantee (coarse). If a layer $W \in \mathbb{R}^{m \times n}$ is element-wise clipped as $|W_{ij}| \leq L_{\text{wc}}$, then

$$\|W\|_2 \leq \|W\|_{\text{F}} \leq \sqrt{mn} L_{\text{wc}}, \quad (105)$$

so a depth- L network with 1-Lipschitz activations satisfies $\text{Lip}(f) \leq \prod_{\ell=1}^L \sqrt{m_\ell n_\ell} L_{\text{wc}}$. This yields at best a *coarse* global bound and often harms capacity. In practice we prefer SN or GP. (Arjovsky et al., 2017; Miyato et al., 2018).

D.5 Other gradient penalties and related methods

- **One-sided GP (Lipschitz penalty).** Penalize only $\|\nabla \tilde{h}_\theta\|_2 > 1$: $\lambda \mathbb{E}[\max(0, \|\nabla \tilde{h}_\theta\| - 1)^2]$, avoiding a push toward < 1 gradients that can reduce capacity (Petzka et al., 2018).
- **Zero-centered penalties R_1/R_2 .** Apply $\lambda \mathbb{E}_{x \sim P_{\text{data}}} \|\nabla_x \tilde{h}_\theta(x)\|_2^2$ (R_1) or $\lambda \mathbb{E}_{x \sim P_g} \|\nabla_x \tilde{h}_\theta(x)\|_2^2$ (R_2) to improve convergence empirically—even though they do not strictly enforce 1-Lipschitzness (Mescheder et al., 2018).

- **DRAGAN (local penalties).** Sample $\hat{x} = x_{\text{real}} + \delta$ with small noise and penalize $\|\nabla_{\hat{x}} \tilde{h}_{\theta}(\hat{x})\|_2$ near the data manifold to promote local smoothness (Kodali et al., 2017).
- **Orthogonal/Parseval constraints.** Constrain $W^T W \approx I$ (Parseval/Björck) to shrink $\|W\|_2$ toward 1 at higher compute cost (Cissé et al., 2017).
- **Lipschitz activations.** Using activations with known Lipschitz constants (e.g., GroupSort) can yield provably 1-Lipschitz networks when combined with spectral control of linear layers (Anil et al., 2019).
- **Optimizer-level gradient clipping.** Stabilizes updates but *does not* impose a function-level Lipschitz bound; . We emphasize that this is different from SN or GP.

These alternatives differ in how strictly they enforce the Lipschitz constraint versus how much computational cost or flexibility they introduce, and we mention them here for completeness.

D.6 Diagnostics and failure modes

We use the following techniques to keep the critic near the 1-Lipschitz regime while preserving capacity and useful gradients to the generator.

- **Monitor gradient norms.** Track the empirical distribution of $\|\nabla_{\hat{x}} \tilde{h}_{\theta}(\hat{x})\|_2$ (for \hat{x} used in the penalty). For WGAN-GP, it should concentrate near 1. Heavy mass $\gg 1$: increase λ or apply the penalty more frequently. Heavy mass $\ll 1$: reduce λ or switch to one-sided GP.
- **Penalty/critic ratio.** Log $\mathbb{E}[(\|\nabla\| - 1)^2]/\mathbb{E}[\text{critic term}]$. Ratios $\ll 10^{-2}$ indicates an ineffective penalty; $\gg 10$ indicates capacity strangling.
- **Check residual branches.** With SN, ensure skip paths are constrained (SN on 1×1 skips or residual scaling); otherwise the global constant can inflate.
- **Avoid BatchNorm in critics.** Batch-dependent statistics interact poorly with gradient penalties and can inject noise into $\|\nabla_x \tilde{h}_{\theta}\|$; use layer/instance norm or none.

E Additional Experimental Results

E.1 CelebA-64 λ_{GP} Sensitivity for BOLT-GAN

For completeness, Figure 4 presents the CelebA-64 λ_{GP} sweep mirroring the CIFAR-10 analysis in the main text. The stability/performance trends are consistent: $\lambda_{\text{GP}} \in [5, 10]$ is best, with variations within ± 1 FID.

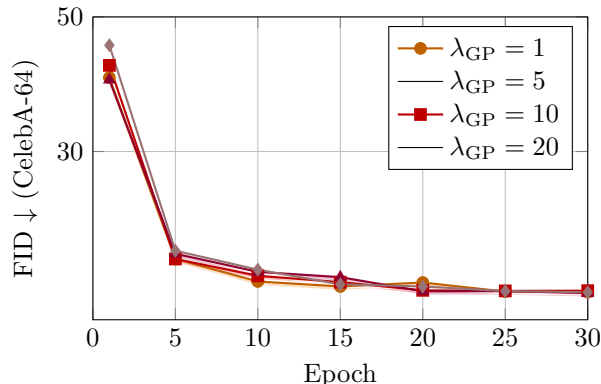


Figure 4: **BOLT-GAN-GP on CelebA-64:** FID vs. epochs for different λ_{GP} values (mean \pm std over 3 seeds). The trend mirrors CIFAR-10: near-optimal, stable performance for $\lambda_{\text{GP}} \in [5, 10]$.

E.2 Qualitative Results

We provide qualitative samples to complement the quantitative results in the main paper: each panel below shows an uncurated 4×4 grid of random images generated by BOLT-GAN-GP after 20 training epochs under the same setup as our primary experiments (same architectures, optimizer, and λ_{GP}).

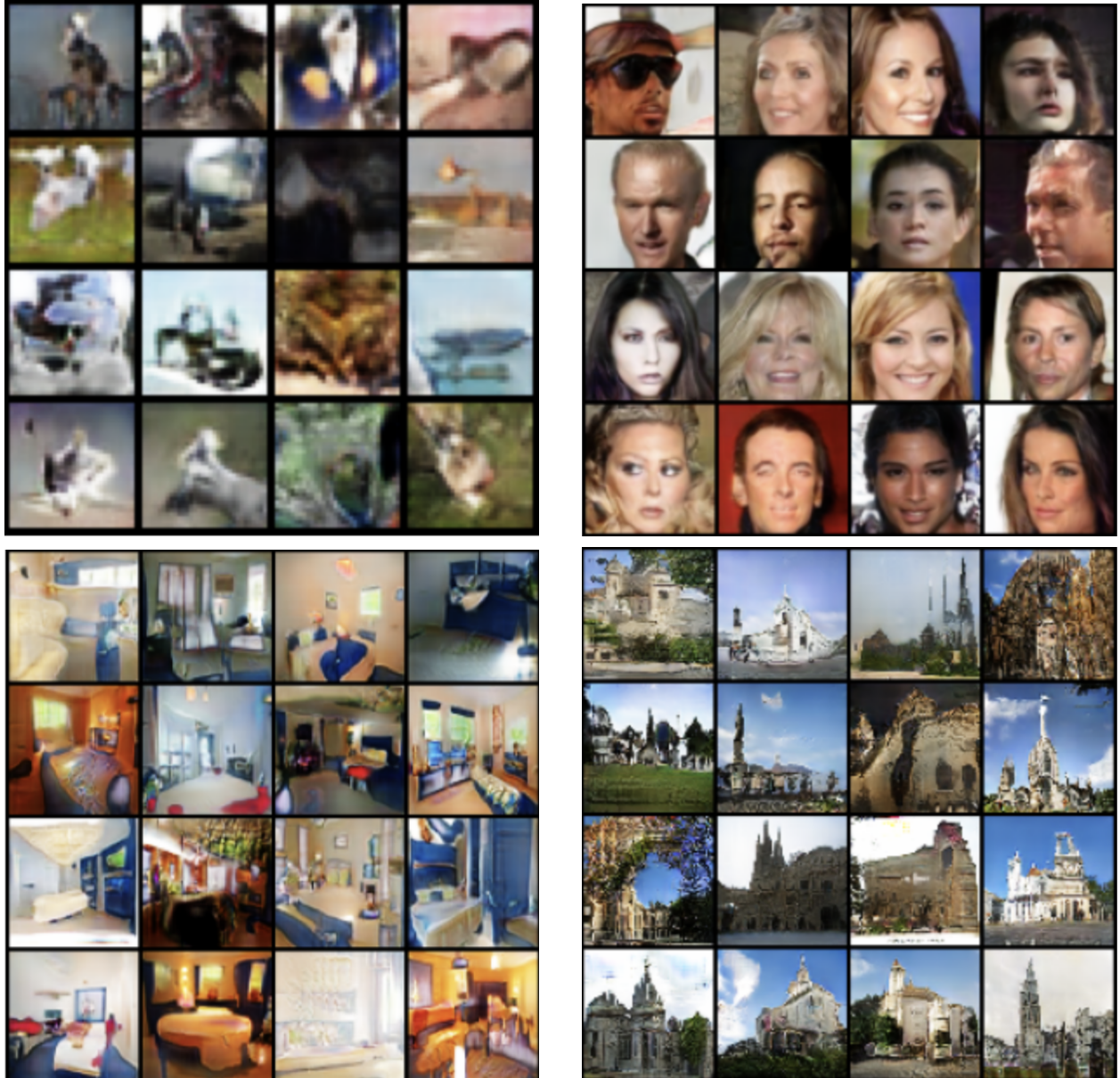


Figure 5: *Qualitative samples (first experiment of the main paper)*. BOLT-GAN-GP after 20 epochs with $\lambda_{\text{GP}}=10$. Top-left: CIFAR-10; top-right: CelebA-64; bottom-left: LSUN Bedroom-64; bottom-right: LSUN Church-64. Each panel shows the same 4×4 grid of generated samples at a reduced scale. Under the identical setup used in our main experiments, Lipschitz BOLT-GAN produces sharper textures, fewer checkerboard artifacts, and more stable color statistics than the WGAN-GP baseline.

F Implementation Details

This section records everything needed to reproduce our results, together with the rationale for each design choice and how the pieces interact (objective, Lipschitz control, optimization, and evaluation). The discriminator produces a raw scalar score $\tilde{h}_\theta(x) \in \mathbb{R}$ and a bounded score $h_\theta(x) = \sigma(\tilde{h}_\theta(x)) \in [0, 1]$ that is used in the BOLT objective. All gradient penalties are applied to the *raw* score \tilde{h}_θ .

F.1 Codebase, Environment, and Hardware

We use Python 3.10+ and the CUDA-enabled build of PyTorch. To improve throughput and reduce memory footprint without affecting FID, we enable automatic mixed precision (AMP) for both networks. When we report “deterministic” runs, we enable determinism switches so that snapshots and sample grids can be reproduced exactly, and we average metrics over multiple random seeds. All experiments were run on NVIDIA A100 GPUs.

F.2 Datasets and Preprocessing

We intentionally keep preprocessing minimal in order to maintain comparability of FID with prior work. Unless otherwise stated, we do not use data augmentation. For **CIFAR-10**, we train at the native 32×32 resolution and normalize images to $[-1, 1]$; for visualization only, we upsample to 64×64 using nearest-neighbor interpolation. For **CelebA-64**, we center-crop faces, resize to 64×64 , and normalize to $[-1, 1]$. For **LSUN Bedroom/Church-64**, we apply a square center-crop, resize to 64×64 , and normalize to $[-1, 1]$.

F.3 Architectures

We adopt a residual DCGAN-style backbone because it offers a good balance between stability and capacity at the 64×64 resolution. The discriminator (critic) does not use BatchNorm in order to avoid interactions with gradient penalties. when spectral methods are used, we treat residual paths carefully.

Generator g_φ (latent $\dim z = 64$). A linear layer projects $z \sim \mathcal{N}(0, I_{64})$ to a $4 \times 4 \times (4 \cdot \text{GF})$ feature map. We then apply a stack of upsampling residual blocks whose depth depends on the target resolution: four blocks for 64×64 (CelebA and LSUN) and three blocks for 32×32 (CIFAR-10).

Discriminator (critic) \tilde{h}_θ . The critic receives images at dataset resolution and applies a stack of down-sampling residual blocks mirroring the generator. For 64×64 , we use four downsampling residual blocks with stride-2 3×3 convolutions (or the standard ResBlockD average-pool projection), two 3×3 convolutions per block, and LeakyReLU activations with negative slope 0.2; the skip path uses a stride-2 1×1 projection. For 32×32 , we use three downsampling residual blocks of the same design. A global sum-pool feeds a linear head that outputs the raw scalar $\tilde{h}_\theta(x)$. Unless otherwise noted, the critic uses no BatchNorm (i.e., we only consider instance or layer normalization in explicit ablations).

F.4 Objectives and Priors

We estimate the prior-weighted BOLT objective on mini-batches using the bounded score $h = \sigma(\tilde{h})$. The critic maximizes the BOLT gap, whereas the generator minimizes it. We set the real/fake prior to $\pi = 0.5$ by default. For $\{x_j\}_{j=1}^B \sim P_{\text{data}}$ and $\{\hat{x}_j\}_{j=1}^B \sim P_g$, let $f_j = \tilde{h}_\theta(x_j)$, $\hat{f}_j = \tilde{h}_\theta(\hat{x}_j)$, $h_j = \sigma(f_j)$, and $\hat{h}_j = \sigma(\hat{f}_j)$. The mini-batch estimator is then

$$\mathcal{L}_{\text{BOLT}}(\varphi, \theta) = \pi \frac{1}{B} \sum_{j=1}^B h_j - (1 - \pi) \frac{1}{B} \sum_{j=1}^B \hat{h}_j.$$

For reference, we also evaluate a non-Lipschitz baseline by setting the gradient-penalty coefficient to zero ($\lambda_{\text{GP}} = 0$). As expected, this variant is numerically unstable and yields high FID; see Sec. S5 for details.

F.5 Lipschitz Enforcement

We enforce approximate 1-Lipschitz behavior of the critic using the WGAN-GP gradient penalty applied to the *raw* score \tilde{h}_θ . Concretely, we sample interpolants $\tilde{x} = \alpha x + (1 - \alpha)\hat{x}$ with $\alpha \sim \text{Unif}[0, 1]$ and add

$$\text{GP} = \frac{\lambda_{\text{GP}}}{B} \sum_{j=1}^B \left(\|\nabla_{\tilde{x}_j} \tilde{h}_\theta(\tilde{x}_j)\|_2 - 1 \right)^2$$

to the critic objective. We set $\lambda_{\text{GP}} = 10$ as our default because this value is the *de facto* choice introduced by WGAN-GP and widely adopted in subsequent implementations; it offers a robust trade-off between stability and capacity in practice (Gulrajani et al., 2017; Mescheder et al., 2018). In Sec. S5 we also report a small sweep over $\lambda_{\text{GP}} \in \{1, 5, 10, 20\}$ that confirms the default is near-optimal under our settings.

F.6 Optimization and Training Schedule

We optimize both networks with Adam using $\beta_1 = 0.5$, $\beta_2 = 0.999$, and learning rates $\eta_d = \eta_g = 2 \times 10^{-4}$. Each iteration performs $n_d = 5$ critic updates followed by one generator update, a ratio that we found to be consistently reliable across datasets. Unless otherwise stated, the learning rate is held constant. We optionally maintain an exponential moving average (EMA) of the generator parameters with decay 0.999 for evaluation, but we leave EMA off by default to match baseline comparisons. The batch size is $B = 64$; when memory is limited, we use gradient accumulation to preserve the effective batch size. Unless otherwise specified, figures correspond to the 20-epoch checkpoint.

F.7 Training Algorithm (Overview and Pseudocode)

Each iteration draws a batch of real samples and a batch of latent codes, produces fake samples, and computes both raw scores \tilde{h} and bounded scores $h = \sigma(\tilde{h})$. We then form the mini-batch BOLT objective, evaluate the gradient penalty along line-segment interpolants, and update the critic by maximizing the BOLT gap (equivalently, minimizing $-\mathcal{L}_{\text{BOLT}} + \text{GP}$). Next, we draw a fresh latent batch and update the generator to minimize the same BOLT gap by reducing the fake-score term. Algorithm 1 summarizes the procedure.

F.8 Hyperparameter Sweeps and Selection

We sweep $\lambda_{\text{GP}} \in \{1, 5, 10, 20\}$ separately for each method and dataset, and we report the best FID per method within a fixed compute budget. Other knobs such as β_1 and n_d have a comparatively minor effect in our ranges (e.g., within ± 1 FID on CIFAR-10).

F.9 Evaluation Metrics

Fréchet Inception Distance (FID). We use FID as the primary quantitative measure of image-generation quality. FID computes the Fréchet distance between multivariate Gaussian embeddings of real and generated images in the feature space of a pre-trained Inception-V3 network (Heusel et al., 2017). Lower values indicate that the generated distribution is closer to the real distribution in terms of both perceptual and statistical similarity. Unless noted otherwise, all FID scores are computed on 50k generated samples using the official Inception statistics for each dataset.

Evaluation Protocol. Unless stated otherwise, we evaluate every checkpoint with 50k samples and the official Inception statistics. Snapshot selection and the choice of λ_{GP} follow the settings detailed in Sec. S7.

F.10 Logging and Diagnostics

We monitor diagnostics that directly reflect Lipschitz control and training health. In particular, we track the empirical distribution of $\|\nabla_{\tilde{x}} \tilde{h}_\theta(\tilde{x})\|_2$ on the interpolants used for the penalty, the value of the penalty term itself, and the ratio $\mathbb{E}[(\|\nabla\| - 1)^2]/\mathbb{E}[\text{critic term}]$. Healthy runs concentrate gradient norms near 1;

Algorithm 1 BOLT–GAN training with gradient penalty (notation matched to paper)

Require: • Discriminator (raw score) \tilde{h}_θ , generator g_φ
 • Data distribution P_{data} , latent distribution P_Z
 • Prior $\pi \in (0, 1]$
 • Batch size B , critic updates per generator update n_d
 • Learning rates η_d, η_g , iterations T
 • Gradient-penalty coefficient λ_{gp}
Ensure: trained parameters θ, φ

- 1: **for** iteration = 1 **to** T **do**
- 2: **for** $k = 1$ **to** n_d **do**
- 3: Sample $\{x_j\}_{j=1}^B \sim P_{\text{data}}$; sample $\{z_j\}_{j=1}^B \sim P_Z$; $\hat{x}_j \leftarrow g_\varphi(z_j)$
- 4: Raw scores: $f_j \leftarrow \tilde{h}_\theta(x_j)$, $\hat{f}_j \leftarrow \tilde{h}_\theta(\hat{x}_j)$; bounded: $h_j \leftarrow \sigma(f_j)$, $\hat{h}_j \leftarrow \sigma(\hat{f}_j)$
- 5: (a) *Batch estimator of $\mathcal{L}_{\text{BOLT}}$ for fixed θ :*

$$\mathcal{L}_{\text{BOLT}}(\varphi, \theta) = \pi \cdot \frac{1}{B} \sum_{j=1}^B h_j - (1 - \pi) \cdot \frac{1}{B} \sum_{j=1}^B \hat{h}_j$$

- 6: (b) *Gradient penalty on raw score (WGAN–GP style):*
- 7: Sample $\{\alpha_j\}_{j=1}^B \sim \text{Uniform}(0, 1)$; $\tilde{x}_j = \alpha_j x_j + (1 - \alpha_j) \hat{x}_j$

$$\text{GP} = \frac{\lambda_{\text{gp}}}{B} \sum_{j=1}^B \left(\|\nabla_{\tilde{x}_j} \tilde{h}_\theta(\tilde{x}_j)\|_2 - 1 \right)^2$$

- 8: (c) *Critic loss & update (maximize $\mathcal{L}_{\text{BOLT}}$):*

$$\mathcal{L}_\theta = -\mathcal{L}_{\text{BOLT}}(\varphi, \theta) + \text{GP} ; \quad \theta \leftarrow \theta - \eta_d \nabla_\theta \mathcal{L}_\theta$$

- 9: **end for**
- 10: *Generator update (minimize $\mathcal{L}_{\text{BOLT}}$):*
- 11: Sample $\{z'_j\}_{j=1}^B \sim P_Z$; $\hat{x}'_j \leftarrow g_\varphi(z'_j)$; $\hat{h}'_j \leftarrow \sigma(\tilde{h}_\theta(\hat{x}'_j))$

$$\mathcal{L}_\varphi = -(1 - \pi) \cdot \frac{1}{B} \sum_{j=1}^B \hat{h}'_j ; \quad \varphi \leftarrow \varphi - \eta_g \nabla_\varphi \mathcal{L}_\varphi$$

- 12: **end for**

persistent mass well above 1 suggests increasing λ_{GP} or applying the penalty more frequently, whereas mass well below 1 suggests reducing λ_{GP} or switching to a one-sided penalty.

F.11 Determinism and Seeds

For exact reproducibility we fix a global seed, propagate per-worker dataloader seeds, and set `torch.backends.cudnn.deterministic=True` and `benchmark=False`. We seed Python, NumPy, and PyTorch random number generators. We release configuration files, grid-reconstruction scripts, and commit hashes that match the figures and tables.

F.12 Failure Modes and Stability Notes

The non-Lipschitz BOLT variant ($\lambda_{\text{GP}} = 0$) frequently diverges or produces very high FID, which is consistent with optimizing a TV-strength objective. Combining strong spectral normalization with a large gradient-penalty coefficient can over-regularize the critic; in such cases we prefer to rely primarily on a single

Lipschitz control. We also avoid BatchNorm in the critic. If the critic saturates, reducing the discriminator learning rate or increasing n_d usually restores stable training. The training code is available in our anonymous repository.